Influence of covariance of aerosol and meteorology on co-located precipitating and non-precipitating clouds over Indo-Gangetic Plains

Nabia Gulistan[1], Khan Alam[1*], Yangang Liu[2]

[1]Department of Physics, University of Peshawar, Peshawar, 25120, Pakistan
[2]Environmental & Climate Science Department, Brookhaven National Laboratory, USA

***Correspondence**: Khan Alam (khanalam@uop.edu.pk)

HIGHLIGHTS

- Strong aerosol-cloud relation under unstable meteorological conditions led to formation of high-level thick clouds.
- In thick clouds the activation of cloud droplets is weakly dependent on aerosols.
- Optically thin clouds led to high precipitation rate.

ABSTRACT

Aerosol-cloud-precipitation-interaction (ACPI) plays a pivotal role in the global and regional water cycle and the earth's energy budget; however, it remains highly uncertain due to the underlying different physical mechanisms. Therefore, this study aims to systematically analyze the effects of aerosols and meteorological factors on ACPI in the co-located precipitating (PCs) and non-precipitating clouds (NPCs) clouds in winter and summer seasons by employing the long-term (2001-2021) retrievals from Moderate Resolution Imaging Spectroradiometer (MODIS), Tropical Rainfall Measuring Mission (TRMM), and National Center for Environmental Prediction/National Center for Atmospheric Research (NCEP/NCAR) reanalysis-II datasets over the Indo-Gangetic Plains (IGP). The results exhibit a decadal increase in aerosol optical depth (AOD) over Lahore (5.2%), Delhi (9%), Kanpur (10.7%) and Gandhi College (22.7%) and decrease over Karachi (-1.9%) and Jaipur (-0.5%). The most stable meteorology with high values of lower tropospheric stability (LTS) is found in both seasons over Karachi. In summer season the occurrence frequency of clouds is high (74%) over Gandhi College, 60% of which are PCs. Conversely, the least number of PCs are found over Karachi. Similarly, in winter season, the frequency of cloud occurrence is low over Karachi and high over Lahore and Gandhi College. The analysis of cloud top pressure (CTP) and cloud optical thickness (COT) indicate high values of cloud fraction (CF) for thick and high-level clouds over all study areas except Karachi. The micro-physical properties such as cloud effective radius (CER) and cloud droplet number concentration (CDNC) bears high values (CER

> ~ 15 µm and CDNC > ~ 50 cm^{-3}) for both NPCs and PCs in summer. The AOD-CER correlation is good (weak) for PCs (NPCs) in winter. Similarly, the sensitivity value of the first indirect effect (FIE) is high (ranged from 0.2 ± 0.13 to 0.3 ± 0.01 in winter, and from 0.19 ± 0.03 to 0.32 ± 0.05 in summer) for PCs and low for NPCs. Sensitivity value for second indirect effect (SIE) is relatively high (such as 0.6 ± 0.14 in winters and 0.4 ± 0.04 in summer) than FIE. Sensitivity values of the aerosol-cloud interaction (ACI) are low (i.e., -0.06 ± 0.09) for PCs in summers. Furthermore, the precipitation rate (PR) exhibits high values in summer season, and PR values are found high in comparatively thin clouds with fewer CDNC (< ~ 50 cm^{-3}) and intermediate for optically thick clouds with higher CDNC (> ~ 50 cm^{-3}).

Keywords: Aerosol-cloud-precipitation-interaction, Aerosol optical depth, cloud effective radius, cloud droplet number concentration, lower tropospheric stability, relative humidity, first indirect effect, second indirect effect, precipitation sensitivity.

1. Introduction

The aerosol-cloud-precipitation-interaction (ACPI) and aerosol-radiation-interaction (ARI) significantly influence climates at the regional and global scales (Romero et al., 2021). Assessing the direct and indirect effects of aerosols is crucial to understand and predict energy budget and the water cycle. In the direct effect, the absorption and scattering of solar radiation by aerosols lead to the warming of the atmosphere and cooling of the earth's surface (Zhou et al., 2020), causing changes in the lower tropospheric stability (LTS) that further leads to modulation of precipitating (PCs) and non-precipitation clouds (NPCs) (Andreae & Rosenfeld, 2008). In the indirect effect, the water-soluble aerosols such as soil dust, sulfates, nitrates, and other organic aerosols ejected naturally and anthropogenically serve as cloud condensation nuclei (CCN) and ice nucleating particle (INP). Hence, aerosols affect the aerosol-cloud-interaction (ACI) by influencing the growth of cloud droplet and cloud droplet number concentration (CDNC) (Twomey et al., 1977; Albrecht, 1989; Jiang et al., 2002; Chen et al., 2011; Tao et al., 2012). The increase of CDNC and decrease of cloud droplet effective radius (CER) inhibit the onset of precipitation and increase the cloud lifetime (Albrecht, 1989). Conversely, the decrease in CDNC and increase in CER increases the probability of precipitation rate (PR). Conversely, Stevens and Feingold (2009) have shown that initially, more sea salt carried by high wind speed inhibit the

precipitation formation. However, the same sea spray tends to seed the coalescence by producing larger CER that led to enhanced precipitation.

In the last few decades, most of the cultivable land of the Indo-Gangetic Plain (IGP) has been replaced by urban developments. Due to the fastest growth of population, urbanization, industrialization, and massive combustion of biomass and fossil fuels in residential homes and factories, a decadal increase in aerosols is observed over IGP. The high aerosol loading may affect the formation of tropospheric clouds and seasonal precipitation patterns (Kaskaoutis et al., 2011; Singh et al., 2015; Thomas et al., 2021) and makes IGP suitable for the study of ACPI. Besides, frequent variations in cloud fraction (CF), extreme precipitation and drought abrupt temperature changes (e.g., heat waves), and irregular unseasonal rains may cause major and unavoidable hazards at local and regional levels in the future.

In the last two decades, the scientific community has focused on quantification of ACI using both observations (Feingold et al., 2003; Costantino et al., 2010; Zhao et al., 2018, 2020; Anwar et al., 2022) and modeling techniques (Chen et al., 2016, 2018; Wang et al. 2020; Zhou et al., 2020; Sharma et al., 2023). Although, a similar recent study (Anwar et al., 2022) attempted to understand the sensitivities of ACI and the first indirect effect of different subsets of AOD to the different conditions of RH and wind directions and found decrease (increase) in CER with aerosol loading known as Twomey effect (anti-Twomey effect) over the monsoon (weak and moderately intensive monsoon) regions. However, the above study excluded the other significant meteorological parameters such as LTS, PR, and T_{850} and was also limited to the monsoon regions of Pakistan only. Further, in the context of warm rain processes, it is generally understood that the high concentration of aerosols capable of serving as CCN leads to enhanced CDNC known as the first indirect effect (FIE) or Twomey effect (Twomey et al., 1977). It is also widely acknowledged that CDNC plays a pivotal role in cloud microphysics and significantly influences the onset of precipitation and retention of water in clouds called the second indirect effect (SIE) (Gryspeerdt et al., 2016; Naud et al., 2017). Whilst, in the above study, the analysis of CDNC is also not addressed. Therefore, the present study aims to deepen the previous study (Anwar et al., 2022), by a long-term and detailed analysis of the ACPI including aerosol-indirect effects for low-level clouds extended over the whole IGP for understanding different mechanisms (condensation, droplet growth and precipitation rate) of cloud and precipitation formation.

This study is focused on estimating the variations in sensitivities of aerosol-cloud relationship to the variations in aerosol loading at specified meteorological conditions for low-level PCs and NPCs in the summer and winter seasons over the IGP. This study is unique in using large number of samples, classification of liquid clouds in PCs and NPCs, further classification of clouds in low, mid, and high-level clouds through joint COT-CTP histograms, quantification of the sensitivities of FIE, SIE, total indirect effect (TIE), and ACI to CDNC. The significant meteorological parameters considered include temperature at 850 hPa, LTS, relative humidity (RH%) at 850 hPa, vertical velocity (Ω), and PR. Furthermore, by utilizing the Moderate Resolution Imaging Spectroradiometer (MODIS) and Tropical Rainfall Measuring Mission (TRMM) data, the correlation of cloud microphysical properties (CER and CDNC) and AOD at specified values of LTS and cloud liquid water path (CLWP) is examined, and precipitation sensitivity at constant macro-physical condition is estimated.

2. Study area and methodology

2.1. Study area

The selected study area (Fig. 1) comprises the upper, middle, and eastern portions of the IGP. The upper part consists of the densely populated and developed regions of the eastern part of Pakistan i.e., Karachi (24.87ºN, 67.03ºE) and Lahore (31.54ºN, 74.32ºE) whereas the middle part comprises the northern part of India i.e., Delhi (28.59ºN, 77.22ºE), Kanpur (26.51ºN, 80.23ºE), Jaipur (26.91ºN, 75.81ºE), Gandhi College (25.87ºN, 84.13ºE), Kolkata (22.57ºN, 88.36ºE), Dhaka (23.80ºN, 90.41ºE) and Patna (25.59ºN, 85.13ºE). The data analysis for the eastern part of IGP (Kolkata, Dhaka, and Patna) is documented as supplementary materials.

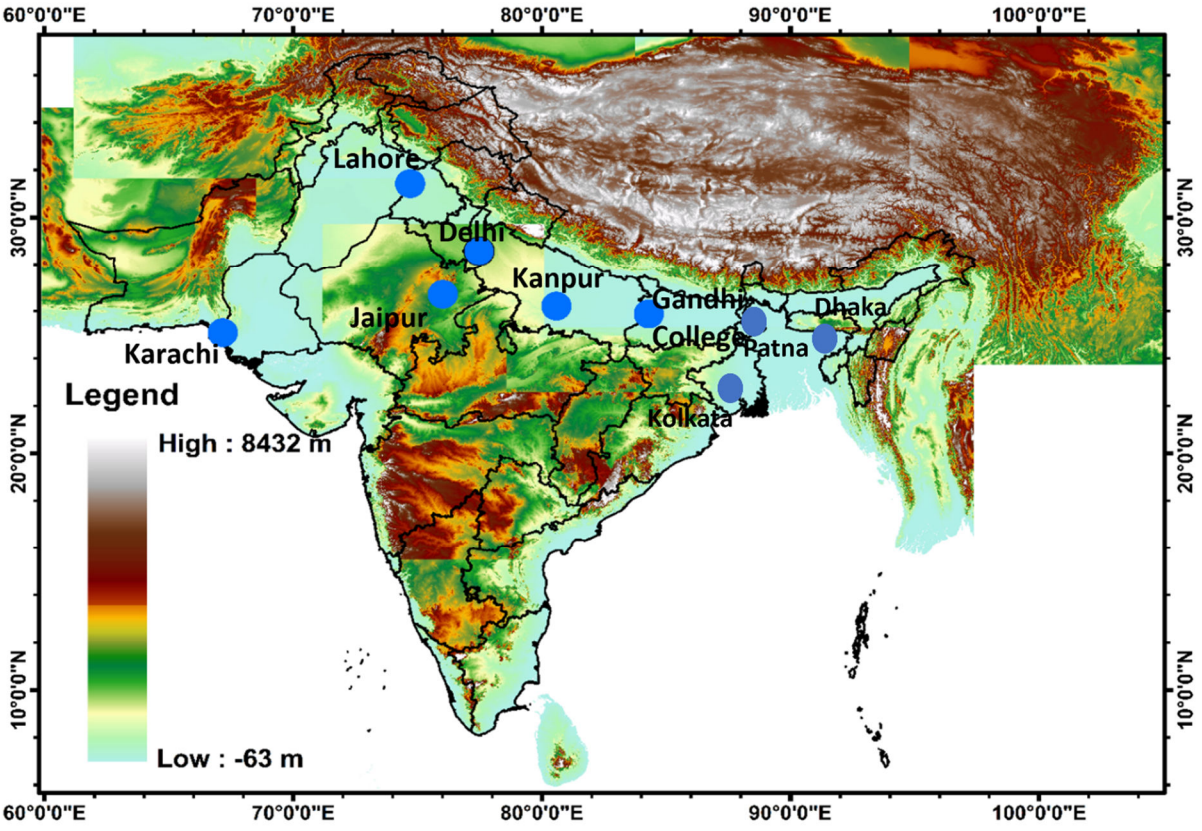

Fig. 1. Topography of the study area.

2.2. Methodology

2.2.1. MODIS, NCEP/NCAR reanalysis-II and TRMM data

Moderate Resolution Imaging Spectroradiometer (MODIS) is a major constituent of NASA's Earth Observing System (EOS). MODIS is orbiting with two onboard satellites, Terra and Aqua, launched in 1999 and 2002 respectively, with a range of 2330 km spanning the entire globe in a day. It provides data and information with a spatial resolution of 1° to study atmospheric processes and physical structure (Kedia et al., 2014; Srivastava et al., 2015). This study uses the daily mean of combined dark target and deep blue AOD at 0.55 μm, cloud top pressure (CTP), cloud top temperature (CTT), CF, CER, and COT for liquid clouds from level 3 aerosol-cloud data product MOD08. Data with AOD > 1.5 are excluded to avoid potential misidentification of aerosols as clouds. The following adiabatic approximation (Brenguier et al., 2000; Wood, 2006; Kubar et al., 2009; Michibata et al., 2014) is used to calculate CDNC (cm^{-3}):

$$\mathrm{CDNC} = \left(\frac{\mathrm{B}}{\mathrm{CER}}\right)^{3} * \sqrt{(2 * \mathrm{CLWP} * \gamma_{\mathrm{eff}})} \quad (1)$$

Where $B = \sqrt[3]{\left(\frac{3}{4}\pi\rho_{water}\right)}$ =0.0620, ρ_{water} is the liquid water density, γ_{eff} is the adiabatic gradient of liquid water content in the moist air column (Wood, 2006). Value of γ_{eff} range from 1 to 2.5 × 10^{-3} at a temperature of 32 K to 104 K (Brenguier, 1991; Zhu et al., 2018; Zhou et al., 2020). The CLWP is estimated by use of

$$CLWP = \frac{5\rho_w(CER)(COT)_w}{9}, \quad (2)$$

Where, ρ_w is the water density at room temperature (Koike et al., 2016).

National Center for Environmental Prediction/National Center for Atmospheric Research (NCEP/NCAR) reanalysis datasets provide global reanalysis data sets that combine satellite observations with the simulation of models through data assimilation (Purdy et al., 2016). Daily data for meteorological parameters including temperature, RH%, and Ω at 850 hPa are retrieved at a spatial resolution of T62 Gaussian grid (1.915° × 1.875°) from NCEP reanalysis-II datasets, and used to calculate lower tropospheric stability (LTS) defined as (Li et al., 2017):

$$LTS = \theta_{700} - \theta_{1000} \quad (3)$$

where θ is the potential temperature and the subscripts denote the pressure levels of 700 hPa and1000 hPa.

The Tropical Rainfall Measuring Mission (TRMM) is the first Joint satellite mission between NASA America and National Space Development Agency (NASDA) Japan, utilizing the visible infrared and microwaves to measure the rain precipitation over tropical and subtropical regions. The main TRMM instruments that are used to measure rain precipitation are precipitation radar (PR) and TRMM Microwave Imager (TMI). Where PR is operating at a frequency of 13.8 GHz and TMI is a passive microwave radiometer consisting of nine channels. A calibrated data set TRMM-2B31 of TRMM Combined Instrument (TCI) for TRMM Multi-Satellite Precipitation Analysis (TMPA) is formed from an algorithm that uses TMI and PR. The product TMPA 3B42 gives the rain precipitation averages on a daily and sub-daily basis. In the current study, the data

product TMPA or TRMM 3B42 is used for the retrieval of PR on daily basis. The spatial resolution of TRMM 3B42 is 0.25º × 0.25º and is available from the year 1998 to till date.

2.2.2. Methodology

The present study is designed to analyze and quantify the ACPI for PCs and NPCs in winter and summer under a variety of meteorological conditions. The daily mean data of each parameter for warm clouds are retrieved from the respective satellites and NCEP/NCAR reanalysis-II for each study site. Subsequently, statistical functions are employed to align the data collected on comparable dates. The data are then segregated into two subsets for the summer and winter seasons. Based on precipitation data from TRMM, the subsets are further divided into precipitating and non-precipitating clouds.

The sensitivities of cloud parameters to CDNC are analyzed through the following formulation considered from previous studies (Zhou et al., 2020):

$$\frac{dln(COT)}{dln(CDNC)} = -\frac{dln(CER)}{dln(CDNC)} + \frac{dln(CLWP)}{dln(CDNC)} \quad (4)$$

In this study, the term on the left side of equation (3) is defined as total indirect aerosol effect (TIE), and the first and second terms on the right side of the equation are defined as the first indirect aerosol effect (FIE), $and\ second\ indirect\ effect\ (SIE), respectively$. Similarly, the sensitivity of CDNC to AOD is evaluated by employing the index of ACI:

$$\mathrm{ACI_{CDNC}} = \frac{dln(CDNC)}{dln(AOD)} \quad (5)$$

The sensitivity of PR to CDNC is calculated from the following equation (Jung et al., 2012) :

$$\mathrm{S_0} = \left(-\frac{\partial ln(PR)}{\partial ln\,(CDNC)}\right)_{COT} \quad (6)$$

3. Results and Discussion

3.1. Regional and seasonal distribution of AOD

AOD is a commonly used proxy for aerosol concentration in the atmosphere and is analyzed here (Fig. 2-3).

IGP characteristically exhibits a diverse and massive pool of aerosols due to its unique topography. The western part of IGP is a coastal location and inlet for the westerly winds. Therefore, dry regions and Arabian sea in the west contribute dust, sea salt and water vapors to the region. The Himalayas in the north act as barriers to the winds, leading to the trapping of aerosols over the central part of IGP. Therefore, this region exhibits a high concentration of anthropogenic aerosols. Bay of Bengal in the east allows southeasterly winds to enter passing across Dhaka, Kolkata, Patna to Delhi and Lahore (Hassan et al., 2002; Anwar et al., 2022). The westerly and easterly winds traverse forested hilly terrain, rivers and lakes elevating humidity level and initiate the cloud formation by activation of the newly originated small aerosol particles as CCNs and cloud formation affecting the local microclimate.

Fig. 2 shows a decadal variation in time average maps for combined dark target and deep blue AOD retrieved at 0.55 μm over the entire study area for the years (2001-2010) and (2011-2021). Also, Table 1 illustrates the percentage change in decadal averaged values of AOD. The results indicate that AOD exhibits a decrease over Karachi (-1.9%) and Jaipur (-0.5%). Whilst an increase in AOD is observed over Lahore (5.2%), Delhi (9%), Kanpur (10.7%) and Gandhi College (22.7%). Similarly, Table 1S shows the decadal change in AOD over Kolkata (18%), Dhaka (22.6%) and Patna (23.3%). Similar to Gandhi College, an increase is observed over all the three areas. Reason for the increase of aerosols include multiple sources of aerosols, human behavior, socio-economic development at local and regional level, and unique topography for persistence and retaining of aerosols.

Fig.3(a-b) shows the probability density function (PDF) for AOD, illustrating different distributions in summer and winter season. Fig.3a shows that the distribution of AOD over Delhi, Kanpur, and Gandhi College is similar. However, a shift in peak value of PDF towards high values of AOD over Lahore and low values over Jaipur illustrate comparatively high and low aerosol concentration in summer season over Lahore and Jaipur respectively. Likewise, Fig. 1S shows the

seasonal PDF values of AOD over Kolkata, Dhaka, and Patna. The results indicate similar seasonal distribution functions over all the three areas of eastern IGP. In both seasons PDF peaks for high values of AOD are observed over Patna showing high concentration of aerosols as compared to Kolkata and Dhaka.

The loading of high concentration of aerosols is owing to the high-density of population, industrialization, and human activities. The major sources of aerosols in all months of the year include vehicular emission originated from old transport facilities, emission of smoke and soot during consumption of biomass for cooking, heavy industrial emission, and aerosols produced in seasonal harvesting and crop-reside burning. All these sources produce organic aerosols which are characterized as hydrophilic particles and have the potential to act as CCN. Likewise, the soil dust particles also act as good CCN due to their hydroscopic nature (Sun & Ariya, 2006). Moreover, the meteorological conditions also play a substantial role to enhance AOD values such as the uplifting of loose soil dust and swelling of aerosols due to holding the water vapors (wv) for long time (Masmoudi et al., 2003; Alam et al., 2010; Alam et al., 2011;). Also, the lower but flat PDF curve demonstrates low values of AOD over Karachi. Ali et al., 2020 associated the low AOD values over Karachi to the westerly and southwesterly winds currents at tropospheric level. However, the decreasing trend in AOD over the coastal city may also be attributed to the variations in other meteorological parameters like T and RH.

As compared to summer season, the pattern of PDF in winter is significantly different as shown in Fig. 3b. The low value of PDF (0.5) for the high value of AOD (0.9) over Karachi illustrates a comparatively pristine atmosphere. Similarly, the PDF peaks for Lahore, Delhi and Jaipur (0.7, 0.7 and 0.8) indicate comparatively high AOD over Delhi. Likewise, the distribution over Kanpur and Gandhi College is similar illustrating similar values of AOD (1.1 and 1.2 respectively). These high values of AOD are attributed to the high emission of anthropogenic aerosols at local and regional level over the central part of IGP (Delhi, Jaipur, Kanpur, and Gandhi College).

Few authors attributed the reduced values of AOD in winter season to the wet scavenging and suppressed emission of aerosols from earth surface (Alam et al., 2010; Zeb et al., 2019). However, in our case, the low (high) values in winter (summer) are associated to dispersion of fine (course) mode particles due to the variations in meteorological conditions.

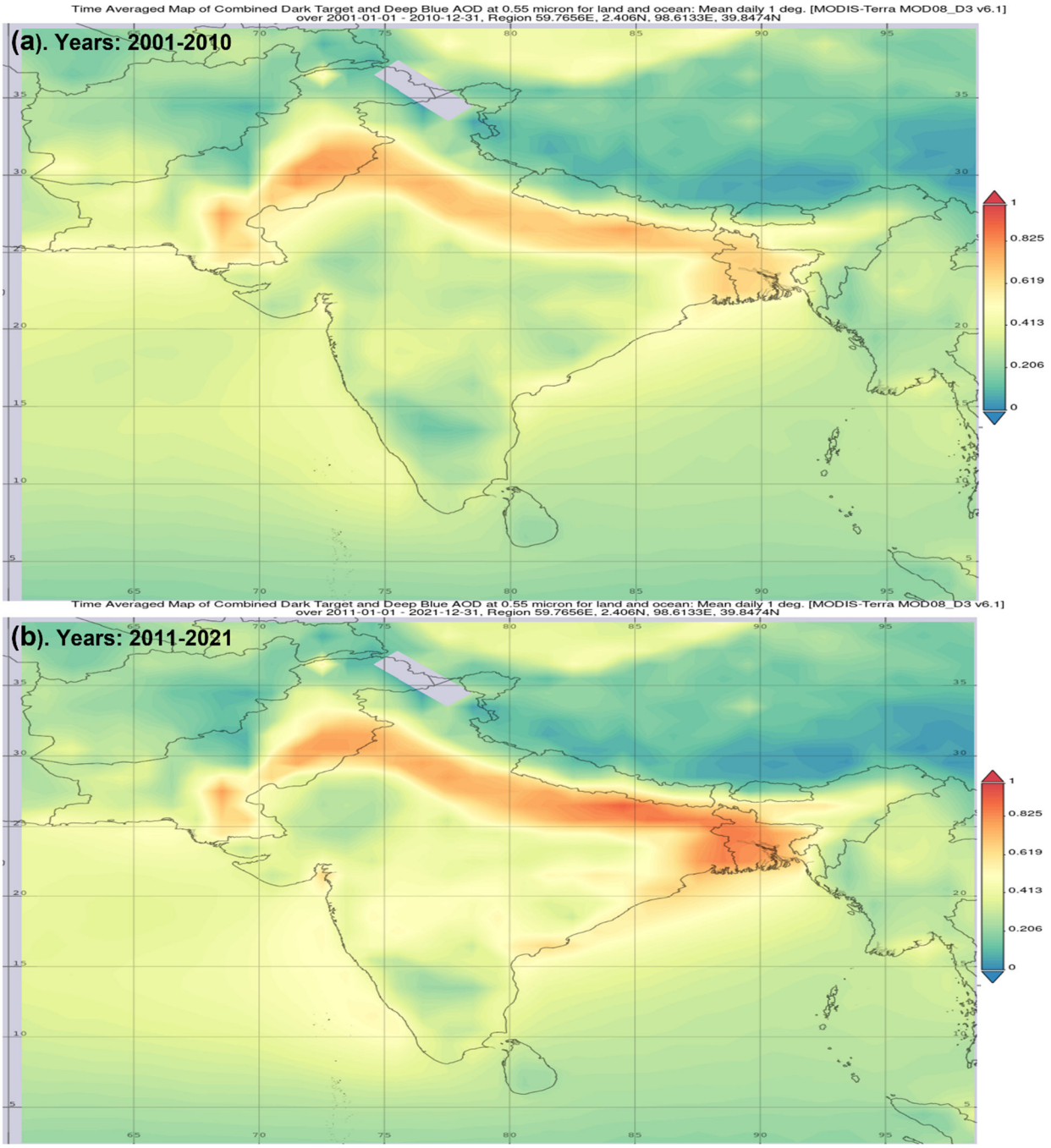

Fig. 2. Decadal increase (year: 2001-2010 and 2011-2021) in AOD over study sites.

Table 1. Decadal percentage variations in average values of AOD over all study areas

	Karachi	Lahore	Delhi	Kanpur	Jaipur	Gandhi College
Total number of counts	5902	6171	5823	5201	5907	5125
Decadal change in AOD	-1.9%	5.2%	9%	10.7%	-0.5%	22.7%

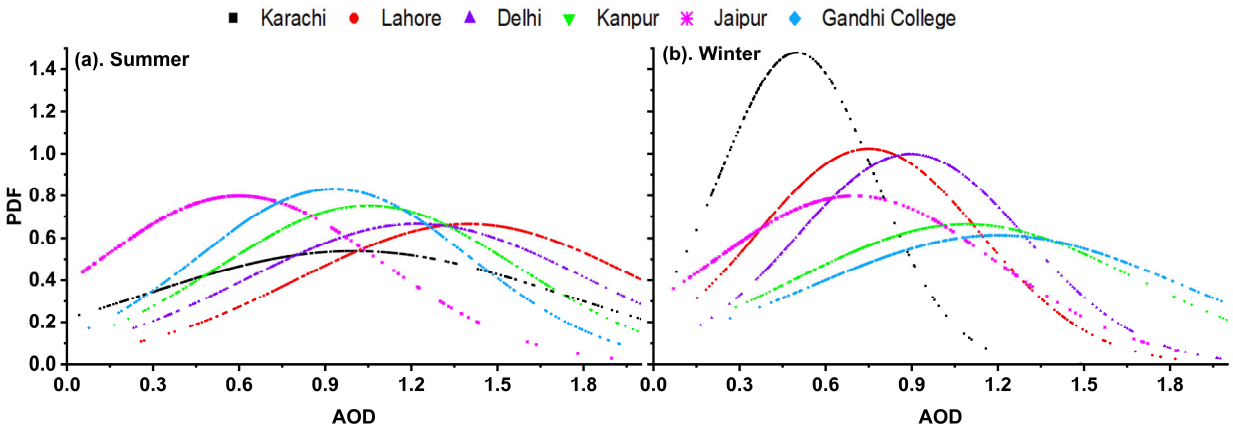

Fig.3. Probability density function (PDF) of AOD over study sites is shown (a) and (b) for summer and winter seasons respectively.

3.2. Climatology of meteorological parameters

Generally, LTS has relationships to factors such as temperature, humidity, wind patterns, and atmospheric pressure over extended periods. It is also widely acknowledged that atmospheric stability, temperature, RH, wind speed, and direction play a significant role in cloud formation (Yang et al., 2015; Tao et al., 2012). Therefore, the influence of long-term variations in the said meteorological parameters are considered in the current study. The variations in meteorological parameters have an unavoidable impact on ACPI. The parameters considered in this study include the temperature, LTS to determine the lower atmospheric stability and instability that influence the process of cloud and precipitation formation through its significant implications on evaporation and convection of the air parcel, the RH% to estimate the level of wv and the Ω to assess the suitable atmospheric dynamics. Fig.4 shows the variations in LTS values for NPCs and PCs in winter and summer season. In winter season, the LTS values are high for NPCs and comparatively lower for PCs over entire study areas. In summer season, the scenario is reversed with high values for PCs but low values for NPCs, suggesting stable tropospheric layer on rainy days. This stabilization may be attributed to the cold pools generated by the evaporation of falling rain

droplets (Wu et al., 2017). The lower LTS values for NPCs in summer season suggest the likelihood of stronger instability that causes high potential of vertical motion and development of thunderstorm. However, Karachi exhibits a distinct pattern of LTS with the highest values in each case, which indicates the existence of the most stable tropospheric layer in Karachi due likely to moist and cold sea breeze due to the city's coastal location.

The remaining meteorological parameters considered in this study are listed in Table 2. The high values in each case are indicated in bold and low values are italicized. The results show that in winter season the temperature at 850 hPa (T_{850}) is relatively high for NPCs ranging from 281±2 K to 286±2 K. The increase in RH% for PCs during winter ranged from (60±5)% to (72±5)%. Also, the $\Omega > 0$ for NPCs and < 0 for PCs in winter season.

In summer season, it is observed that T_{850} is comparatively higher than that for the winter clouds and ranged from 298±0.4 to 300±0.7 K and 296±0.5 to 298.3±0.6 K for NPCs and PCs respectively. The high values of T_{850} are due to intense solar fluxes in summer season that keep the temperature of the earth's surface and adjacent atmospheric layer higher. Also, the increase in RH% during summer ranged between 25-45 %. The reason for the high values of wv and RH% is mainly the suitable thermodynamical conditions such as evaporation and convection due to the high temperature of earth surface and air (Sherwood et al., 2010). The results show high values of RH% 72 ± 5 (71.6 ± 3) in winter (summer) season for PCs over Gandhi College. Conversely, notable fluctuations in RH% are observed over the coastal city, Karachi, with values of 70 ± 13.9 (68.4 ± 6.7) in winter (summer). Similarly, Fig. 2S and Table 2S show the LTS conditions for PCs and NPCs. The high LTS values indicate more stable condition over Dhaka. Similarly, Table 2S shows the seasonal average values for other meteorological parameters. The results indicate high values of T_{850}, RH% and Ω **297.5±1.1(297.5±1.4)**, **82.1±16.8(76.3±19.7)** and **-0.2±0.1(-0.17±0.1)** respectively for PCs (NPCs) for over Patna in summer.

Besides, during the last two decades, the wv and fog over the Arabian Sea were increased (Verma et al., 2022). Therefore, the high values of wv and RH% in summer months is due to the high-speed zonal winds that blew in the summer season and transport water vapors and sea salt from the surface of the Arabian Sea and hydrophilic aerosols such as soil dust from deserts of Iran, Pakistan, and India to IGP. Moreover, during the winter season, the elevated humidity levels are noticeable over IGP, particularly in the vicinity of Gandhi College. This increased humidity is a

result of evapotranspiration driven by agricultural practices, irrigation, the presence of rivers and lakes, and the introduction of moist, cold air from western winds (Nair et al., 2020). Where $\Omega < 0$ for PCs over all study areas except Karachi.

The distinct variations in meteorological parameters reveal the occurrence of clouds with diverse properties. The detailed analysis of such clouds is given in the next subsections.

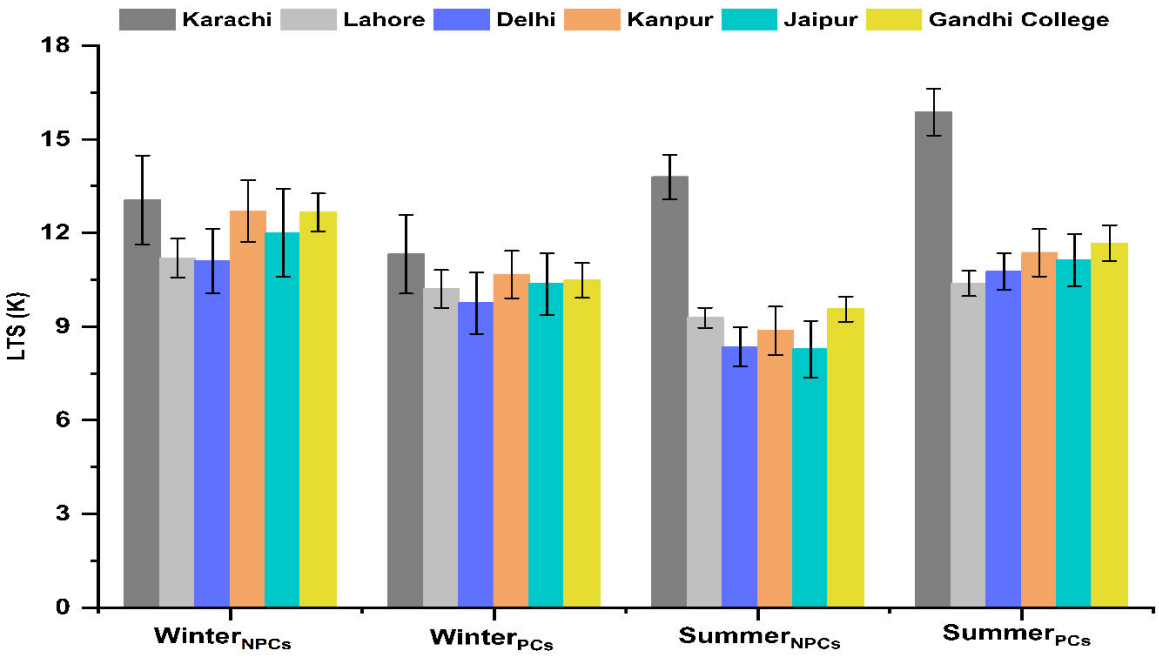

Fig. 4. Variations in lower tropospheric stability (LTS) over all study sites for PCs and NPCs in winter and summer seasons, the error bars show the standard deviation (SD) values.

Table 2. Meteorological parameters for PCs (NPCs) in summer and winter seasons. Maximum values are for both types of clouds shown in bold and minimum values are indicated as italic.

	Winter Season			Summer Season		
	T_{850} (K)	RH%	Ω (m/s)	T_{850} (K)	RH%	Ω (m/s)
Karachi	*278±18* (**286±2**)	70±13.9 (38.3±9)	*-0.04±0.04* (*0.030.02*)	*296±0.5* (299±0.84)	68.4±6.7 (45.4±6.2)	*0.02±0.04 (-5E-05±0.02)*
Lahore	280.5±1 (*281±2*)	*60±5* (36.9±4.4)	*-0.04±0.04*(**0.07±0.02**)	**298.3±0.6**(**300±0.7**)	*63.6±5.2* (*35±4.4*)	*-0.02*±0.02 (*0.03*±0.02)
Delhi	282.5±0.9 (283±0.9)	60.3±9 (35.2±5)	-0.12±0.04(0.04±0.03)	297.4±0.6(299.3±0.8)	64.5±3 (42.5±5.5)	*-0.05*±0.03 (*0.003*±0.02)
Kanpur	284.3±0.5 (284±0.8)	64.1±4 (37±5)	**-0.15±0.03**(0.04±0.04)	297±0.6(298.4±0.7)	70.4±5 (46.5±6)	*-0.12*±0.03 (***-0.07*±0.03**)
Jaipur	**284.4±1.3** (284±1)	67.5±6 (**40.4±7**)	-0.08±0.02(0.04±0.02)	296.7±0.8(299±0.9)	64.9±3 (50.6±4.2)	*-0.03*±0.02 (*-0.03*±0.01)
Gandhi College	283.3±0.5 (284.3±0.7)	**72±5** (*31.6±5*)	-0.12±0.05(0.05±0.03)	297±0.4(*298±0.4*)	**71.6±3** (**54±4**)	***-0.16*±0.03** (*-0.01*±0.03)

306 ### 3.3. Regional and seasonal distribution of clouds and precipitations

307 #### 3.3.1. Regional and seasonal differences in clouds occurrence and its microphysical
308 structure

309 Fig.5 shows the frequency of occurrence of precipitable clouds and total number of cloudy
310 days. Chen et al. (2018) suggested the COT to be the effective measure for assessing the clouds
311 and potential for precipitation. In our case, to avoid any overestimation, the COT data are
312 aligned with PR data on corresponding dates and then filtered to include COT ~ > 5 for PCs.
313 The results show that in the winter season the frequency of clouds is low over Karachi and high
314 over Lahore and Gandhi College. The results suggest the high number of PCs only over Lahore.
315 In summer season, the high number i.e., 74 % of the total data counts over Gandhi College are
316 identified as cloudy days, 60 % of which are PCs. Similarly, most of the clouds over Lahore,
317 Delhi and Jaipur are PCs. Conversely, the least number of PCs (6 %) are found over Karachi.
318 Likewise, Fig. 3S shows the total number of cloudy days and the number of days on which PCs
319 occurred. The high occurrence of clouds is observed over Kolkata 83% (60%) and Dhaka 91%
320 (69%) in summer (winter) season. The high occurrence of PCs in summer is due likely to the
321 significant impact of elevated aerosols with the southwesterly winds on the summer monsoons
322 and occurrence of PCs. Therefore, Kolkata and Dhaka are of critical importance from
323 perspective of aerosol loading and ACI (Dahal et al., 2022).

324

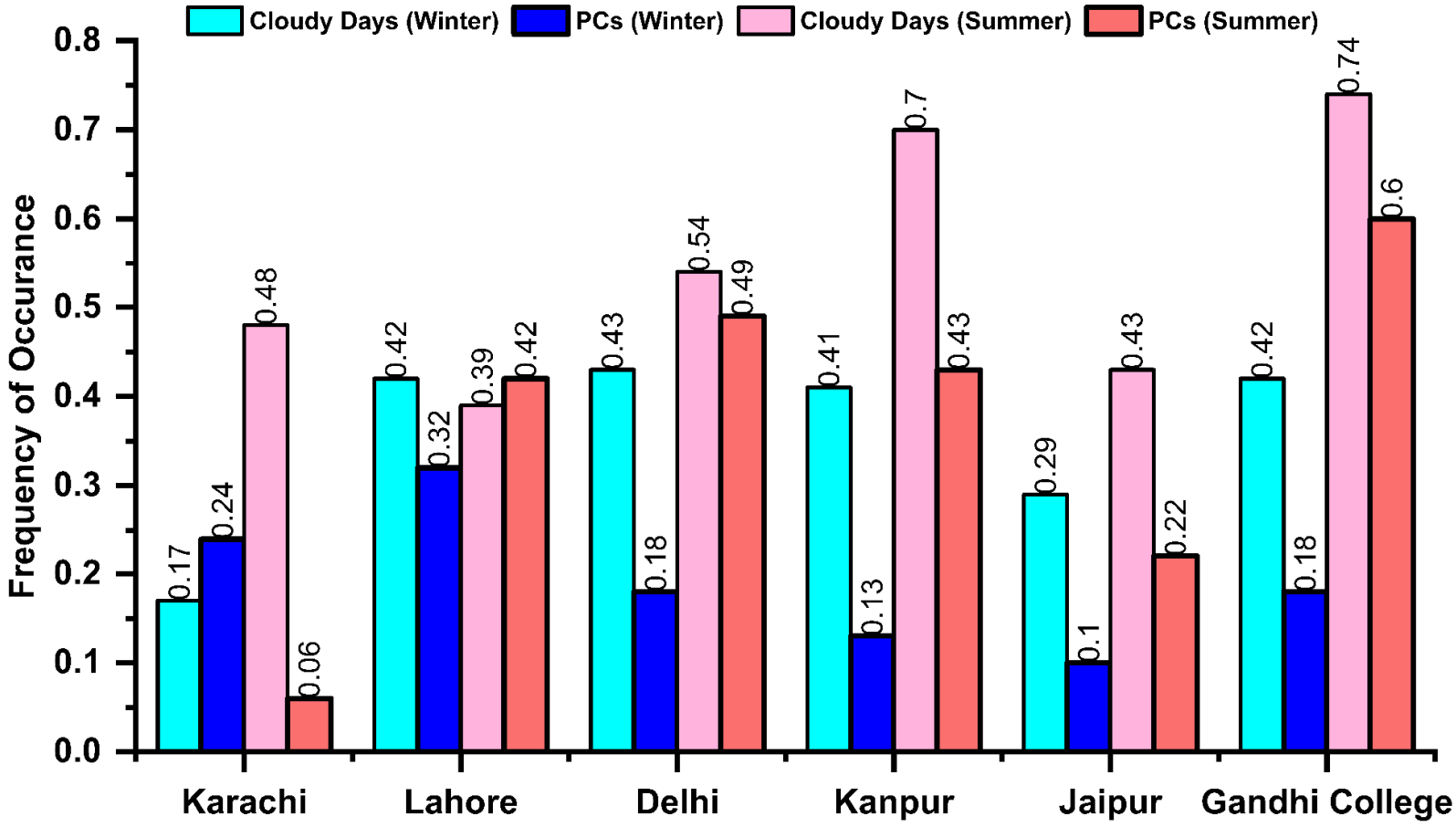

Fig. 5. Frequency of occurrence of total cloudy days (including PCs and NPCs) and only PCs is shown for both winter and summer seasons.

Table 3 shows the criteria adopted from previous papers (Rossow & Schiffer, 1999; Wyant et al., 2006; Sharma et al., 2023) for further classification of NPCs and PCs into different type of clouds. The aim of identifying the cloud types is to assess the cloud regimes and their vertical structure for the better understanding of ACPI. In accordance with table 3, Fig. 6 shows joint histograms of COT-CTP displaying the median values of CF for nine different types of clouds. For a quick visual comparison, the cloud types are ordered from low to high level clouds. Also, for each histogram, the bins of COT and CTP are located on x- and y-axis respectively. While the CF of each bin is represented with the colored bar with its value mentioned in the histograms as shown in Fig. 6.

The results exhibit noticeable differences in the pattern of cloud regimes over all study areas. The diverse CF values are observed in winter and summer seasons for NPCs and PCs over Karachi. In winter season, only stratus NPCs ($23 < COT < 60$, $800 > CTP > 680$ hPa) are dominant with CF ~ 0.9. While, in summers, high value of CF ~ 0.9 for low and intermediate thickness of high-level clouds such as Cirr-Stratus NPCs ($3.6 < COT < 23$, $180 < CTP < 440$ hPa) are observed. Similarly, the type of PCs in both summer and winter season that occurred with CF ~1.0 include cirrus and cirr-stratus. The relatively reduced value of CF for thick NPCs in winters and PCs in summers is attributed to the low values of AOD and high values of LTS. The results depicted slight differences and similarities in CF values for thick and thin NPCs respectively in winter season for all areas except Karachi. Besides, the high-level PCs are identified in the two bins of CTP ($180 < CTP < 440$ hPa) and ($440 < CTP < 680$ hPa) over all study areas. The formation of these similar types of PCs in winters are associated with the similarities in Ω, LTS values and aerosols concentration.

Likewise, in summer season, the matrices of PCs and NPCs exhibit a wide range of cloud types. However, the CF values are comparatively high for PCs. Most of the identified PCs are formed in the two bins of CTP, ($180 < CTP < 440$ hPa) and ($440 < CTP < 680$ hPa) with CF values ranging from 0.8 to 1.0. The results suggest low values of CF for the low-lying thick NPCs over all study areas. Moreover, the results illustrate a more frequent occurrence of all the three types of thick NPCs in one bin of COT ($23 < COT < 60$) and all the three types of high-level NPCs for CTP ($180 < CTP < 440$ hPa) over Delhi, Kanpur, and Gandhi College. Therefore, these are considered the cloudiest regimes. Besides, contrasting regional variations are also observed in PCs. The maximum CF values for all types of PCs are observed over Kanpur and Gandhi College. Similarly, relatively good values of CF in a bin of COT ($23 < COT < 60$) and

a bin of CTP (180 < CTP < 440 hPa) over Lahore, Delhi, and Jaipur depict the frequent occurrence of thick and high-level PCs, respectively. In addition, among all the estimated low-level PCs, cumulus and strato-cumulus exhibit good CF values (0.7) over Kanpur and Gandhi College. The formation of thick clouds can be attributed to the enhanced convection process due to the atmospheric instability.

Table 3. Classification of clouds based on CTP – COT joint histograms.

	COT		
CTP (hPa)	0-3.6	3.6-23	23 to >60
440 to <180	Cirrus	Cirr-Stratus	Deep convection
680-440	Alto-Cumulus	Alto-Stratus	Nimbo-Stratus
<800 to 680	Cumulus	Strato-Cumulus	Stratus

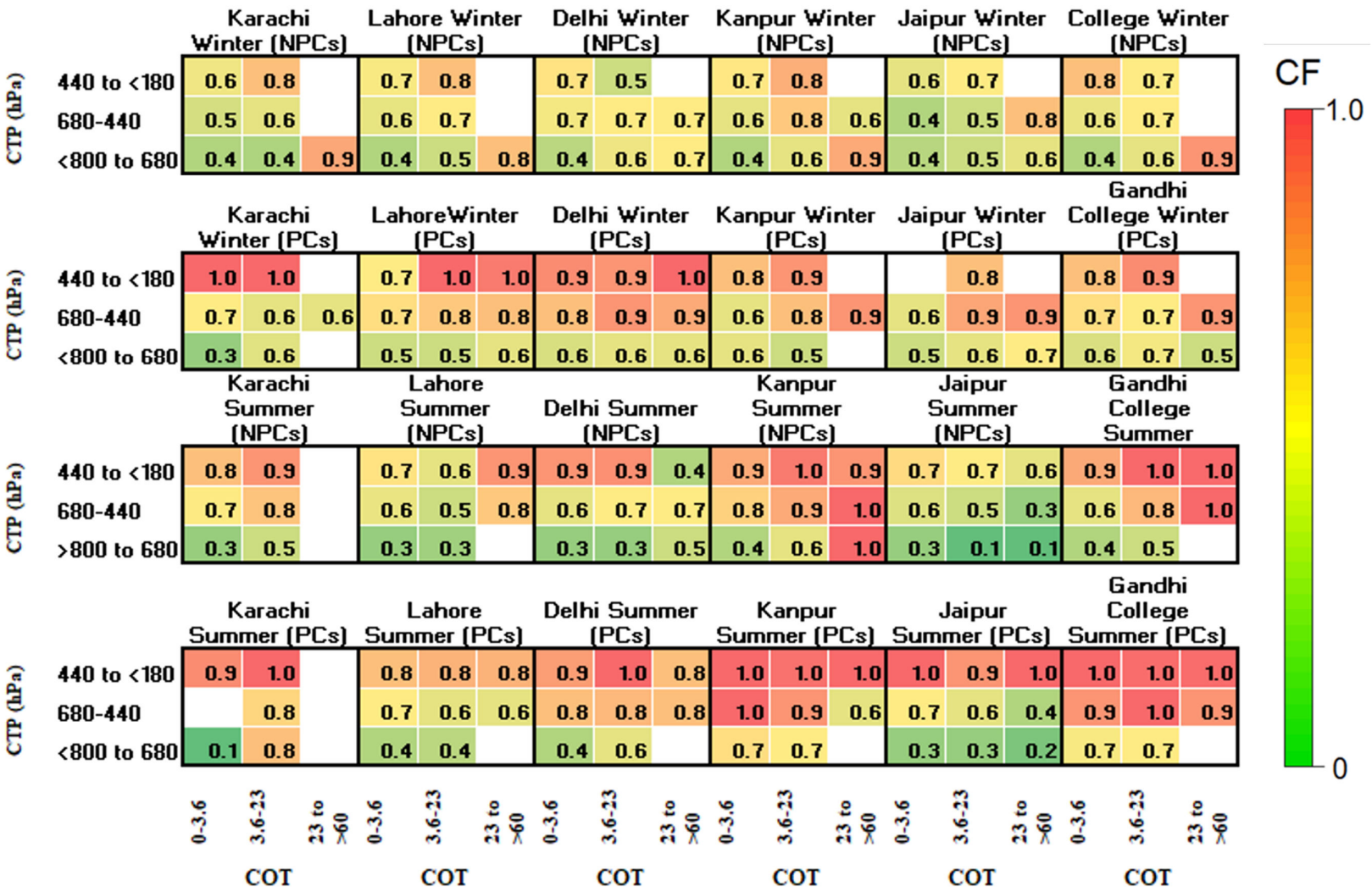

Fig. 6. Types of NPCs and PCs in winter and summer season

After estimating the cloud types, Fig. 7 shows the probability distribution function (PDF) of cloud microphysical properties for the identification of differences in microstructure of NPCs and PCs in summer and winter seasons. From the results it is depicted an approximately similar pattern for the CER of NPCs in winter. However. the clouds have high peaks of PDF for lower values of CDNC over Karachi. The low number of CDNC results in thin NPCs as shown in Fig.7. Similarly, Fig. 7(c and g) shows the microstructure of NPCs in summer. The results indicate that as compared to CER values in winter, the probability of CER >~15 μm is high in summer season. However, high peak for CER < 15 μm is observed over Karachi. Similarly, the CDNC shows a high probability for CDNC > 50 cm^{-3} with the high PDF values over Karachi. Where, the lowest number of CDNC is observed over Lahore indicating the formation of high-level thin NPCs in summer.

Fig. 7(b and f) shows the distribution pattern of CER and CDNC of PCs in winter season. It is clearly observed that the distribution of CER for PCs is like those for NPCs in winter season. However, PDF have peak values for relatively higher CDNC, which illustrates the occurrence of thick clouds. Fig. 7(d and h) shows the variations in CER and CDNC in summer season. The results show a wider distribution for CER > ~15 μm and higher peaks for CDNC > ~ 50 cm^{-3} suggesting the formation of thick PCs in summer as shown in Fig.6.

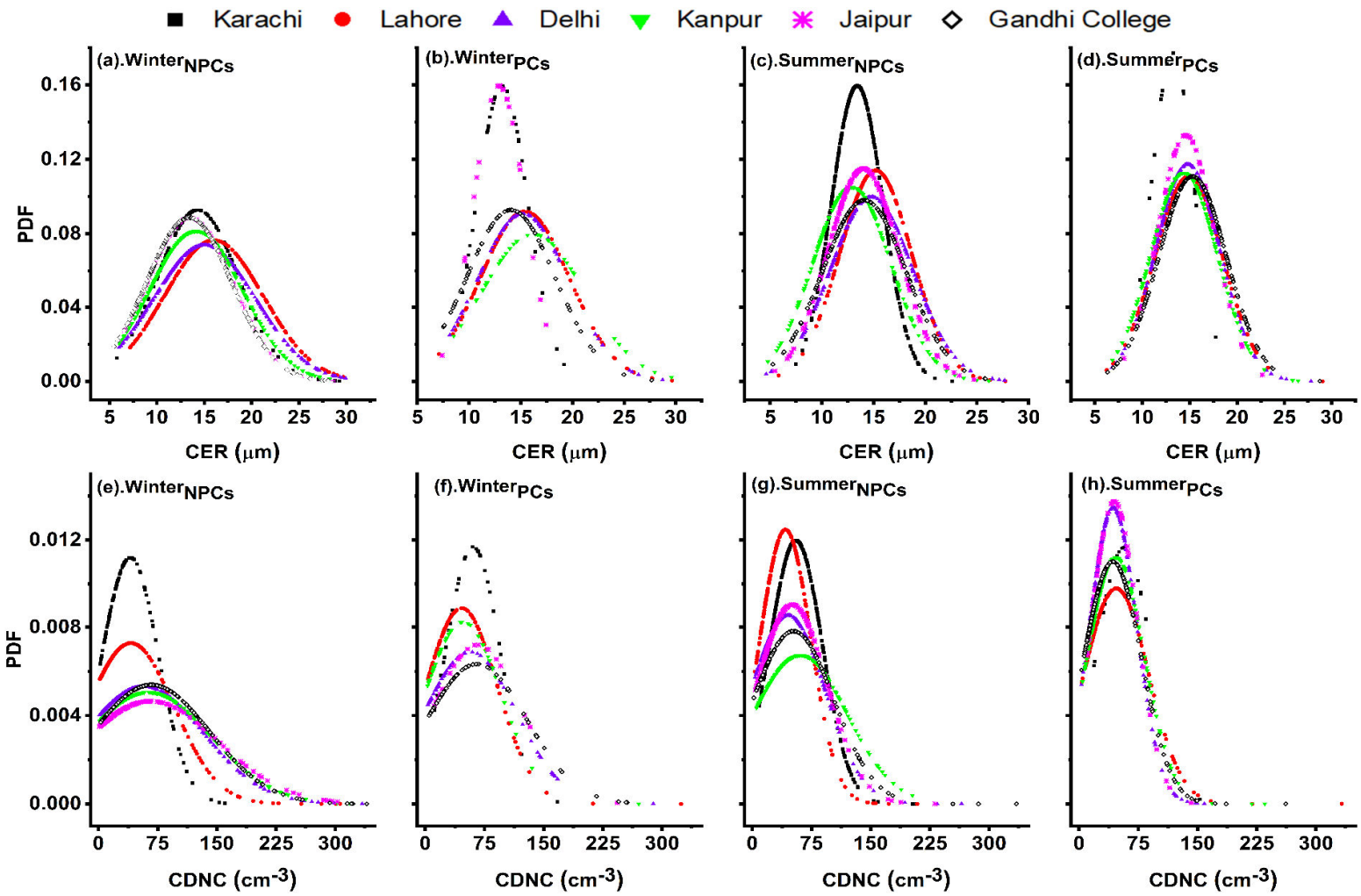

Fig. 7. Probability density function (PDF) of precipitating (PCs) and non-precipitating clouds (NPCs) in winter and summer season

3.4. Aerosol-Cloud-Precipitation Interaction (ACPI)

In the following sections, ACPI is analyzed and discussed in detail for PCs and NPCs in summer and winter seasons.

3.4.1. Aerosol effects on cloud properties

The impact of aerosols on CDNC and CER of PCs and NPCs is illustrated as scatter plots in Fig. 8-9. The quantification of the AOD-CER and AOD-CDNC relationships is demonstrated through detailed linear regressed slopes, regression coefficients (R^2) and Pearson's correlation coefficient (R). The color bar represents the variations in LTS. Fig.8 shows that in winter season, the AOD-CER correlation is good for PCs and weak for NPCs. The results also show that the LTS values are higher for NPCs. The weak AOD-CER correlation may be linked to the inhibition of droplet growth due to less soluble aerosols, originated from biomass burning (Kang et al., 2015). In our case, all the selected study areas are among the most urbanized and industrialized areas of IGP. Therefore, most of the prevailing aerosols are the less soluble soot and BC particles. That weakened activation of cloud droplets inhibits the formation of PCs and evaporates to higher altitudes and thereby increases the droplet residence time (Kumar & Physics, 2013). Besides, the results show a contrasting pattern of LTS values. Although, RH over Karachi (38.3±9 %) is higher than over the other study areas (shown in Table 2), the negative AOD-CER correlation is observed over Karachi due to its coastal location, the low value of AOD and high level of LTS.

Fig. 9 illustrates the AOD-CER and AOD-CDNC correlation in summer season. The results depict a more significant and positive AOD-CER correlation in summer season than winter season. Unlike winter season, the high LTS values are observed for PCs. Yuan(2008) associated the positive AOD-CER correlation to the soluble organic aerosols. Myhre et al. (2007) hypothesized that the positive AOD-CER correlation is a maximum for low CTP and minimum for high CTP. Hence, in our study, referable to the approximated CF values shown in Fig.6, the significant and positive AOD-CER correlation under unstable atmospheric conditions resulted in thick and high-level clouds. Furthermore, it is observed that CER and CDNC values for NPCs increase with increasing instability. Meanwhile, the enhanced process of droplet activation may result in large AOD, higher CER, giant and fewer CCN (Yuan, 2008). Therefore, the weak correlation of AOD with CER and CDNC may be due to the anthropogenically ejected water-soluble organic aerosols and a smaller number of CCN.

Fig. 5S and 6S show the impact of AOD on CER and CDNC for PCs and NPCs in winter and summer respectively. The results indicate a positive and weak AOD-CER correlation 0.2, 0.07 and 0.004 for NPCs over Kolkata, Dhaka, and Patna respectively and for PCs (0.08) over both Kolkata and Patna. Similarly, a positive and weak AOD-CDNC is observed over all areas for PCs. Likewise, Fig. 6S also illustrates weak AOD-CER correlation is 0.06, 0.2 and 0.12 for both types of clouds in summer. As compared to other areas, the correlation analysis is less significant over Karachi, Kolkata, Dhaka and Patna. This can be attributed to the persistence of diverse aerosol types influenced by their coastal locations, different meteorology and the alternating inflow and outflow of easterly and westerly winds.

Recent advances in remote sensing led to cost-effective solutions and an increase in available data at various temporal and spatial resolution to bridge scientific gaps among different disciplines. While satellite-based retrievals have many advantages over in-situ and ground-based measurement such as broader regional coverage and enhanced spatial resolution, they are still prone to considerable uncertainties owing to the indirect nature of remote-sensing, retrieval algorithms, thermal radiance, infrequency of satellite overpasses, and cloud top reflectance (Hong et al., 2006; Tian et al., 2010; Hossain et al., 2006). In our study, apart from the aforementioned factors contributing to the uncertainty, any residual cloud contamination could also lead to biased retrieval of AOD. Likewise, satellite-based retrievals for cloud properties are crucial to understanding the pivotal role of clouds in climate and the role of clouds is still a dominant source of uncertainty in prediction of climate change. These, uncertainties in AOD and retrievals of cloud properties also propagate through the modeling process, potentially leading to less accurate climate predictions. Likewise, these uncertainties appeared to influence the findings in the current investigation. For instance, a limited correlation between AOD and CER is observed over Lahore, particularly in cloudier regimes as depicted in Fig. (5-6). This contrasts with robust impacted documented in the earlier studies (Michibata et al., 2014). However, high sensitivity of SIE is observed for PCs particularly in winter season indicating the delay in onset of precipitation and more retention of clouds.

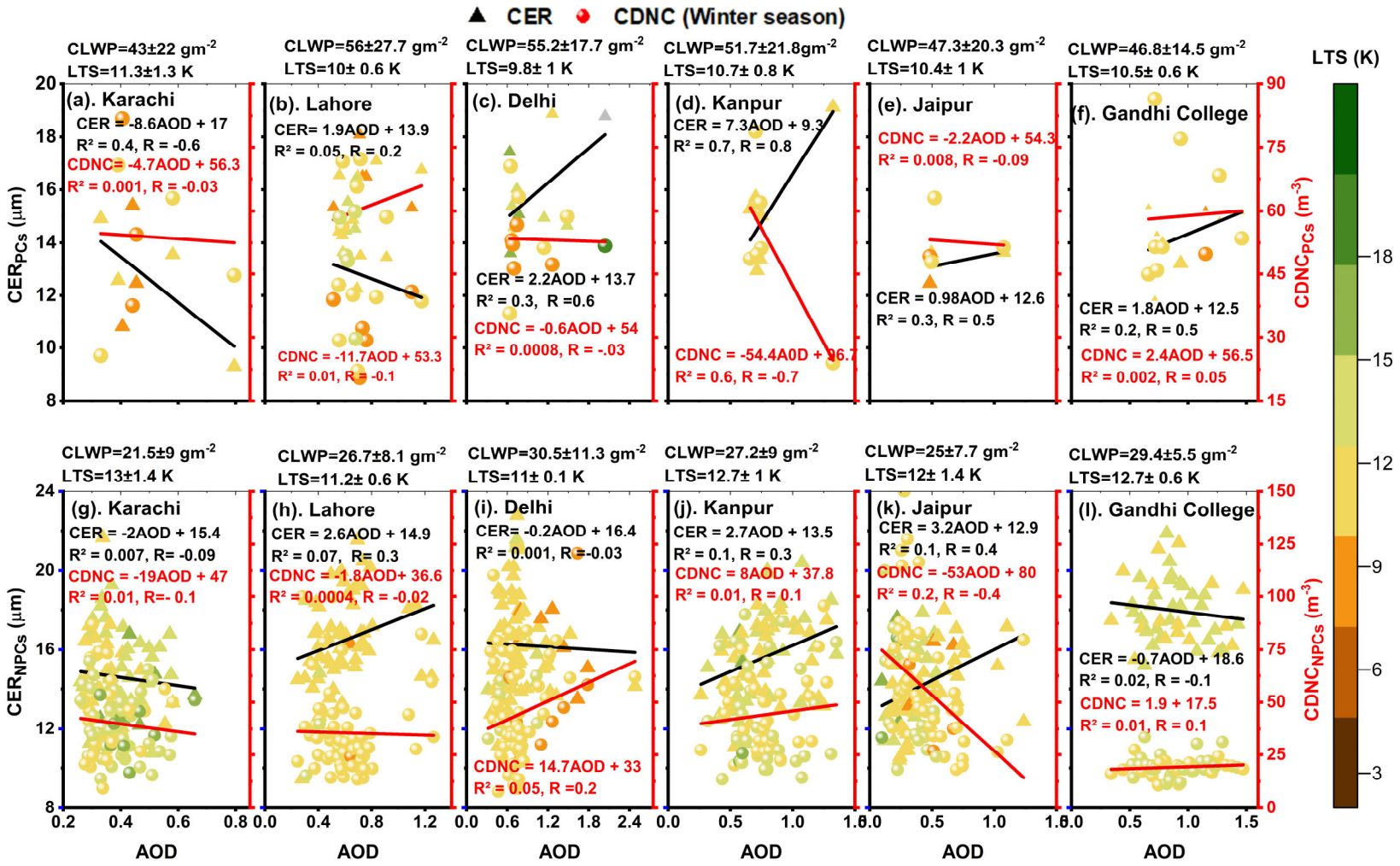

Fig. 8. AOD-CER and AOD-CDNC regression and correlation coefficient for PCs and NPCs over all study areas in winter season.

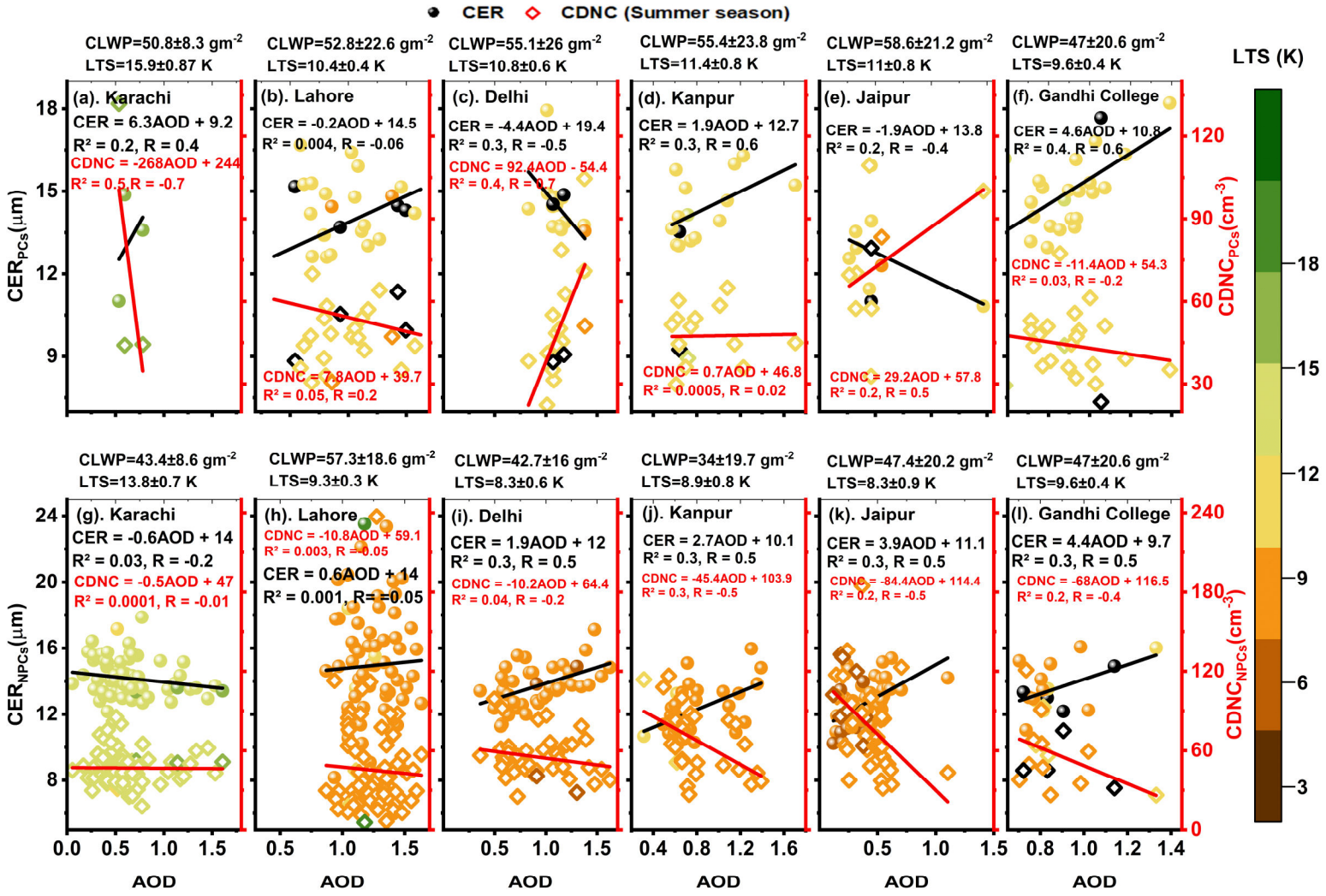

Fig. 9. Same as Fig. 8 but in summer season.

3.4.2. *Seasonal variations in sensitivities of aerosol-cloud indirect effects and ACI*

Fig.10 shows assessment of four ACI sensitivities in terms of CDNC using daily mean values of MODIS observations available over the entire study area. Since studying the effects of aerosols on the co-located clouds is a challenging task due to the overestimation of thin clouds in AOD retrievals. Therefore, to minimize the propagation of AOD retrieval errors in ACI, the current study attempted to estimate the sensitivities of different cloud mechanisms to CDNC.

The sensitivity of CER to CDNC is assessed as a signature of FIE as shown in Fig.10a. The positive values illustrate that CER decreases with an increase in CDNC revealing the occurrence of the Twomey effect. Whilst the negative values depict the anti-Twomey effect. Tripathi et al., (2007) divided IGP into four regions as western, central, eastern part of IGP and the foothills of Himalayas. Their results depicted high concentration of dust in western part, and an increase in anthropogenic aerosols as one moves from western to eastern part of IGP. Therefore, they attributed the resulted strong indirect effect in winter to the high concentration of regional anthropogenic pollution. However, in our case, the FIE is investigated for both PCs and NPCs in both seasons. The resulted approximations in winter season show strong (weak) sensitivity of FIE for PCs (NPCs). Similarly, the estimated sensitivity of FIE for all NPCs and PCs is also positive in the summer season. Fig. 7S(a) shows sensitivities for FIE in both seasons for PCs and NPCs. The results indicate high values of sensitivity FIE in winter season which is similar to the results for Karachi, Lahore, Delhi and Kanpur as shown in Fig. 10 a. This is attributed to high level of aerosol emission from residential heating and industrial activities. Furthermore, the results illustrate higher values of FIE in summer. This is attributed to the massive aerosol loading due to aerosol carried by winds and originated by anthropogenic activities and unstable meteorology.

Fig. 10b illustrates the sensitivity of CLWP to CDNC as a proxy for evaluation of the SIE or lifetime effect. The positive sensitivity estimated for all NPCs and PCs suggested that the CLWP increase with increase in aerosol. Further, the results show that the sensitivity of SIE is stronger for PCs in winter which indicates the delay in onset of high PR. Similarly, the results show that the SIE sensitivity values are higher for PCs than for NPCs in the corresponding seasons. Therefore, the results depict that the lifetime of PCs is greater than NPCs. Which is attributed to the high level of RH for PCs as shown in Table 2. Fig. 10 (a and b) shows that the FIE sensitivities are weaker than SIE.

Fig. 10c shows the TIE in terms of the sensitivity of COT to CDNC. The results illustrate positive values of sensitivity for all NPCs and PCs which indicate that COT increases with increase in aerosol concentration. The results also reveal that sensitivity of TIE is a linear sum of the sensitivities of FIE and SIE. Further, the results also suggest that the variations in TIE sensitivity are largely dependent on SIE.

Fig.10d shows the sensitivity of CDNC to AOD as an estimation of ACI in terms of CDNC. The positive values show the increase in CDNC with the increase in AOD. Therefore, positive ACI reflects the inhibition of precipitation formation. Whilst the negative values illustrate the decrease in CDNC and enhanced PR (Fan et al., 2018). The results depicted relatively large and positive sensitivities for NPCs in winter over Lahore, Delhi, and Kanpur, which inhibits the onset of rainfall. The Sensitivity of ACI for NPCs in summer is positive over Karachi and Lahore and negative over Delhi, Kanpur, Jaipur, and Gandhi College. Ackerman et al. (2004) associated the negative ACI_{CDNC} to the wet scavenging and mixing of air by entertainment. In our case, negative ACI may be due to the growth of CER and decrease in CDNC with aerosol loading under unstable conditions (shown in Fig. 9). Further, the magnitude of sensitivity for PCs in summer is low. Which can be due to the droplet growth through collision coalescence and wet scavenging in thick clouds, decreased dependency on CCN.

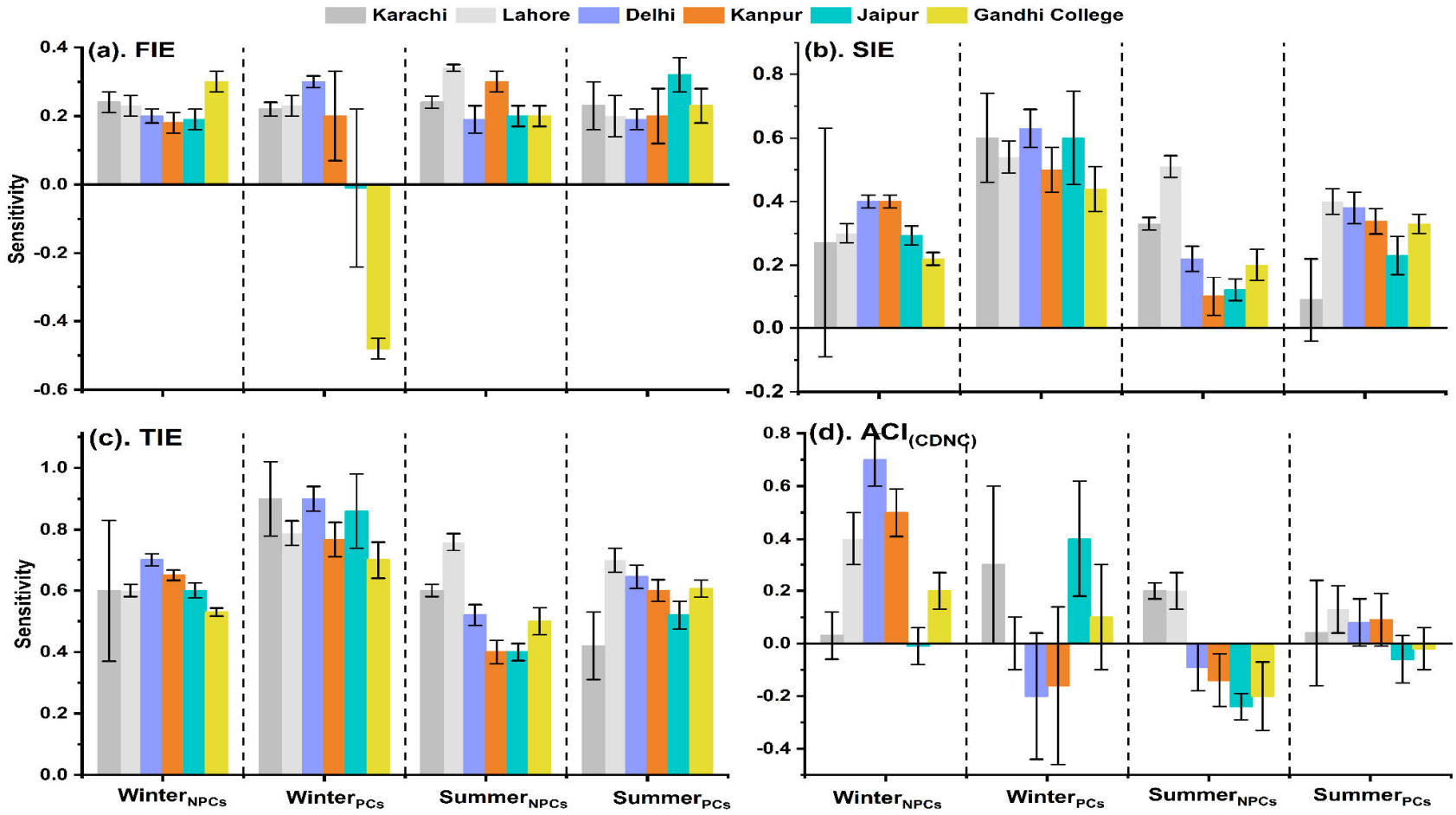

Fig. 10. The sensitivity metrices estimated for aerosol-cloud relationship using CDNC is shown in (a) FIE = $-\left(\frac{\partial ln\,(CER)}{\partial ln\,(CDNC)}\right)$ (b) SIE = $\left(\frac{\partial ln\,(cLWP)}{\partial ln\,(CDNC)}\right)$, (c) TIE = $\left(\frac{\partial ln\,(COT)}{\partial ln\,(CDNC)}\right)$ and (d) ACI = $\left(\frac{\partial ln\,(CDNC)}{\partial ln\,(AOD)}\right)$. Where, the error bars show the standard deviation (SD).

3.4.3. Aerosol effects on precipitation

Fig. 11 shows the average values of PR in mm/day retrieved from TRMM. The results show an obvious seasonal difference in precipitation occurrence. The reason for the high (low) PR values is due to the suitable meteorological condition including high (low) LTS values for PCs in summer (winter) season (shown in Fig. 8-9). The stable atmospheric condition with high LTS value in winter serves to inhibit the convection process and have a significant impact on controlling the PR in winter (Zhao et al., 2006). Conversely, during summer season, the meteorological instability prevails with low LTS values which result in high RH. This not only causes enhanced AOD due to the water uptake and resulted swelled hydrophilic aerosols (Alam et al., 2010; Alam et al., 2011) but also affects the cloud and precipitation formation due to the enhanced evaporation and convection. Additionally, Fig. 8-9 also show evidently and specifically during summer that the possible cause of positive AOD-CER correlation is the negative AOD-CDNC correlation under unstable meteorology over all areas except Karachi. As a result, Fig. 11 shows high (low) values of PR over all areas with maximum over Gandhi College (Karachi). The results show high (low) approximation of PR over Gandhi College (Karachi). Knowing that the rate of conversion of CDNC to precipitation is proportional to CER (Wolf & Toon, 2014). Therefore, the high PR values is due to the growth of bigger cloud droplets in summers. Further, apart from the reasons mentioned in the preceding sections, the other justification for the differently perturbed aerosols, clouds, and precipitation pattern over the study areas in summers is due to the entrance of southeast winds from Bay of Bengal passing across Gandhi College to Delhi and Lahore and entrance of same winds from Arabian sea to Pakistan through Karachi (Anwar et al., 2022).

Fig. 12 shows scatter plots of PR verses CDNC. The plot is colored with COT to examine the impact of CDNC on PR for similar macrophysics. When CDNC are few, then the COT are sparse that grow larger, form less reflective clouds and precipitate faster (Kump & Pollard, 2008). The same phenomenon seems true in our case. The results illustrate high PR (0.0007 mm/day) values for clouds with COT ranging from 3 to 28 with CDNC $< \sim 50$ cm^{-3} and intermediate for optically thick clouds and CDNC $> \sim 50$ cm^{-3} in both seasons.

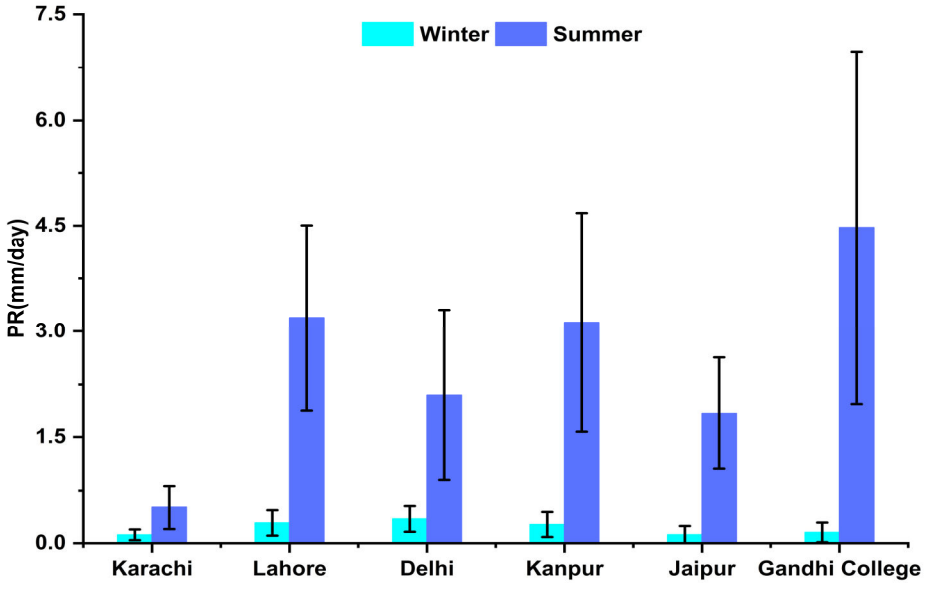

Fig. 11. Mean Precipitation rate (PR) for the PCs in winter and summer season and SD values with 95% confidence interval.

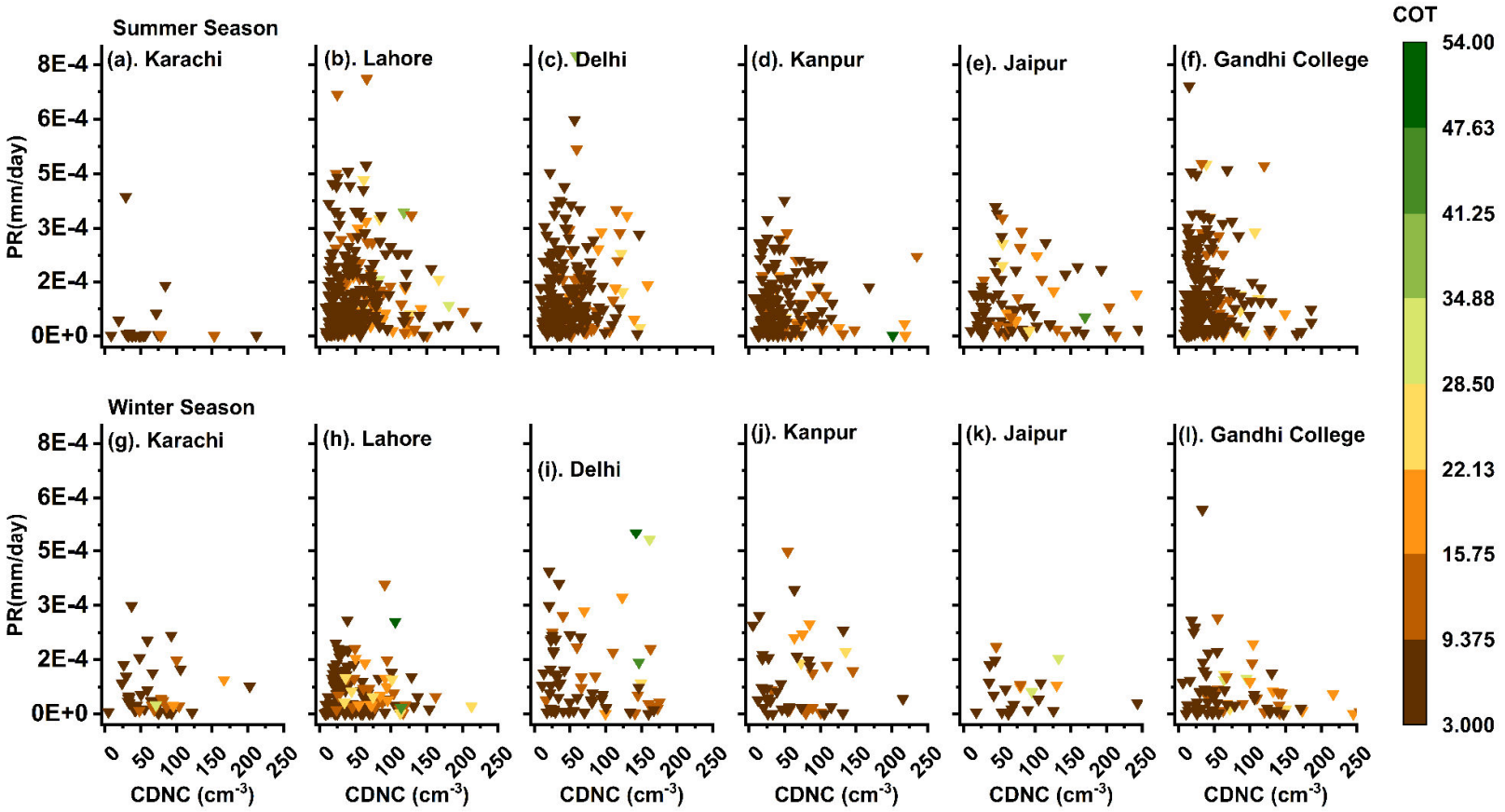

Fig. 12. Scatter diagrams of PR (mm/day) verses CDNC (cm^{-3}) in summer and winter seasons. color coding shows the COT of PCs.

Fig.13 shows the sensitivity (S_o) of PR to CDNC defined by $S_o = \left(-\frac{dln(PR)}{dln\,(CDNC)}\right)_{COT}$ for clouds of low and intermediate thickness illustrated in Fig. 13 a and Fig. 13 b respectively. However, sensitivity analysis for COT > 23 could not be performed due to less number (0 to 04) of available samples. In the sensitivity equation the minus sign shows the suppression of precipitation formation due to the increase in CDNC. Further, when S_o is positive, correlation between PR and CDNC is negative; however, for negative S_o, PR and CDNC are positively correlated. The results show peak values of S_o i.e., 0.7 ± 0.3, 0.6 ± 0.3, 0.5 ± 0.3, and 0.4 ± 0.4 over Jaipur, Delhi, Gandhi College and Karachi respectively at intermediate values of COT in winter, indicating the occurrence of lightly precipitating clouds. Referable to Fig. 13b, the low magnitude of S_o 0.2 ± 0.3 and 0.08 ± 0.2 over Kanpur and Lahore respectively is due to coagulation, in which precipitations are less sensitive to CDNC.

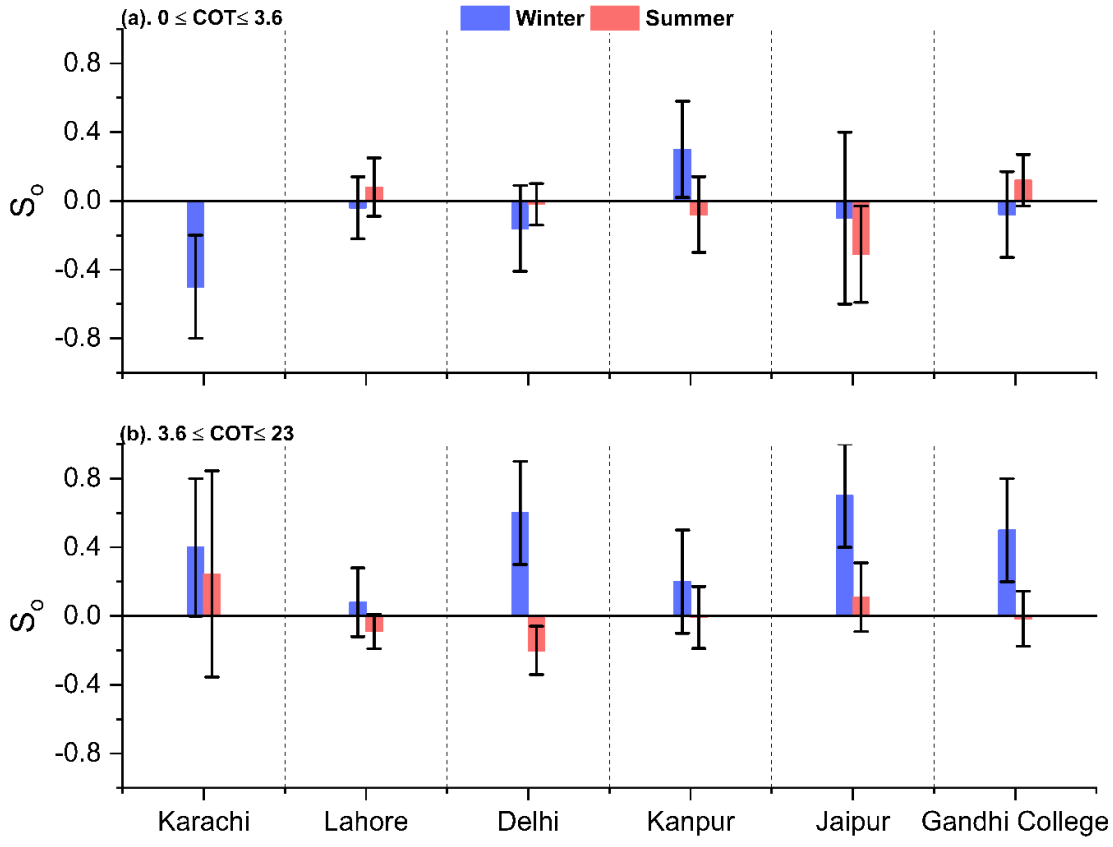

Fig. 133. Sensitivity 'So' of precipitation rate (PR) for two bins of COT shown in (a). 0 ≤ COT ≤ 3.6 and (b). 3.6 ≤ COT ≤ 23.

4. Conclusion

In this study, the long-term (2001-2021) data retrievals from MODIS coupled with TRMM and NCEP/NCAR reanalysis-II datasets over the entire study area are compiled and analyzed for PCs and NPCs in winter and summer season. The following are the main findings of this study.

A decadal decrease in AOD is observed over Karachi (-1.9%) and Jaipur (-0.5%). Meanwhile, AOD exhibits an increase over Lahore (5.2%), Delhi (9%), Kanpur (10.7%) and Gandhi College (22.7%). The LTS values are High (low) for NPCs (PCs) in winter and for PCs (NPCs) in summer season. However, among all study areas, Karachi exhibits comparatively high LTS values in both seasons. Apart from that, the increase in RH% for PCs ranged from 33-57% in winter and from 25-45 % in summer. $\Omega > 0$ for all NPCs in winter and < 0 for PCs in both winter and summer seasons.

In winter season low frequency of cloudy days over Karachi and high over Lahore and Gandhi College is estimated. Also, the high number of PCs are estimated only over Lahore. In summer season, out of the 74 % of the cloudy days, 60 % are PCs over Gandhi College. Similarly, most of the clouds over Lahore, Delhi and Jaipur are PCs. Conversely, the least number of PCs (6 %) is found over Karachi. The high-level PCs are identified in one bin of CTP ($180 < CTP < 440$ hPa) over all study areas in winters. In summer season, all the three types of high level and thick PCs have significant values of CF. The low-level PCs are identified as stratus clouds. Further, PDF values for CER $> \sim 15$ μm and CDNC $> \sim 50$ cm^{-3} for NPCs and PCs is high (low) in summer (winter) over all areas except Karachi.

The AOD-CER correlation is good for PCs and weak for NPCs in winter season. Also, the CER and CDNC values increase with increase in LTS. The sensitivity value of FIE is high (low) for PCs (NPCs) in winter. Further, magnitude of sensitivity of FIE (SIE) is low (high). Also, the sensitivity of TIE is a linear sum of the sensitivities of FIE and SIE. Further, ACI sensitivity values for PCs in summer are small, illustrating less dependency of CER on CDNC in thick clouds.

The high (low) PR values are observed in summer (winter). Further, high PR values for comparatively thin clouds with fewer CDNC $< \sim 50$ cm^{-3} and intermediate for optically thick clouds and CDNC $> \sim 50$ cm^{-3} are observed. Sensitivity values are small (high) for thick clouds in summer (winter).

Being one of the major source regions of anthropogenic aerosols across the globe, IGP offers interesting insights into the study of ACPI coupled with aerosol indirect effects. This study highlights that the aerosol-cloud relationship exhibits different behavior under different meteorological conditions, at coastal and inland locations. Thus, compared to other study areas, the stable atmospheric conditions due to the constant sea breeze weakened the ACI over Karachi, which resulted in a smaller number of CDNC, NPCs, and PCs. Further, our study also provides a very good platform for the detailed analysis of sensitivity tests of aerosol indirect effects and precipitation formation.

Limitations and future recommendations:

Although the current study is as thorough as possible, however, it has its limitations due to the topographical complexity of IGP, the lack of in-situ measuring instruments in Pakistan, and the intrinsic uncertainties associated with satellite-based data. Therefore, simulations of ground-based measurements along with satellite-based retrievals and calculation of cloud properties and CCN by different Community Atmosphere Model (CAM) and Weather Research and Forecasting (WRF) Models are recommended for deep insight into the various mechanisms of ACPI over IGP.

Data Availability: The MODIS and TRMM data can be obtained from the NASA Goddard Earth Sciences Data and Information Center (GES DISC) and can be retrieved from the websites: https://modis.gsfc.nasa.gov/data/ and https://gpm.nasa.gov/data . The reanalysis-II datasets are obtained from the website: https://psl.noaa.gov/data/gridded/data.ncep.reanalysis2.html . The processed data used in this work are available on reasonable request from the corresponding author.

Author contribution: NG processed and analyzed the data and wrote the original draft of the manuscript. KA proposed the Idea, supervised this work and revised the manuscript. YL helped in revising the manuscript.

Acknowledgment: The authors gratefully acknowledge the NASA Goddard Earth Sciences Data and Information Services Center (GES DISC) for the provision of freely available data retrieved from MODIS and TRMM. We are also grateful to the NOAA Physical Sciences Laboratory (PSL) for free accessibility to (NCEP/NCAR) reanalysis-II datasets.

References

Ackerman, A. S., Kirkpatrick, M. P., Stevens, D. E., & Toon, O. B.: The impact of humidity above stratiform clouds on indirect aerosol climate forcing, *Nature.*, *432*, 1014-1017, https://doi.org/10.1038/nature03174 , 2004.

Alam, K., Iqbal, M. J., Blaschke, T., Qureshi, S., & Khan, G.: Monitoring spatio-temporal variations in aerosols and aerosol–cloud interactions over Pakistan using MODIS data, Adva. Space Res., *46*, 1162-1176, https://doi.org/10.1016/j.asr.2010.06.025, 2010.

Alam, K., Qureshi, S., & Blaschke, T.: Monitoring spatio-temporal aerosol patterns over Pakistan based on MODIS, TOMS and MISR satellite data and a HYSPLIT model, Atmos. Envi., *45*, 4641-4651, https://doi.org/10.1016/j.atmosenv.2011.05.055, 2011.

Albrecht, B. A.: Aerosols, cloud microphysics, and fractional cloudiness, Sci., *245*, 1227-1230, https://doi.org/10.1126/science.245.4923.122 , 1989.

Ali, G., Bao, Y., Ullah, W., Ullah, S., Guan, Q., Liu, X., . . . Ma, J.: Spatiotemporal trends of aerosols over urban regions in Pakistan and their possible links to meteorological parameters, Atmo., 11, 306, https://doi.org/10.3390/atmos11030306, 2020.

Andreae, M., & Rosenfeld, D.: Aerosol–cloud–precipitation interactions. Part 1. The nature and sources of cloud-active aerosols, Earth. Sci. Rev., *89*, 13-41, https://doi.org/10.1016/j.earscirev.2008.03.001, 2008.

Anttila, T., Brus, D., Jaatinen, A., Hyvärinen, A. P., Kivekäs, N., Romakkaniemi, S., & Lihavainen, H.: Relationships between particles, cloud condensation nuclei and cloud droplet activation during the third Pallas Cloud Experiment, *Atmos. Chem. Phy.*, *12*, 11435-11450, https://doi.org/10.5194/acp-12-11435-2012 , 2012.

Anwar, K., Alam, K., Liu, Y., Huang, Z., Huang, J., & Liu, Y.: Analysis of aerosol cloud interactions with a consistent signal of meteorology and other influencing parameters, Atmos. Res., *275*, 106241, https://doi.org/10.1016/j.atmosres.2022.106241, 2022.

Brenguier, J.-L., Pawlowska, H., Schüller, L., Preusker, R., Fischer, J., & Fouquart, Y.: Radiative properties of boundary layer clouds: Droplet effective radius versus number concentration, Atmos. Sci., *57*, 803-821, https://doi.org/10.1175/1520-0469(2000)057<0803:RPOBLC>2.0.CO;2 , 2000.

Chen, F., Sheng, S., Bao, Z., Wen, H., Hua, L., Paul, N. J., & Fu, Y. : Precipitation Clouds Delineation Scheme in Tropical Cyclones and Its Validation Using Precipitation and Cloud Parameter Datasets from TRMM, Applied Met. Climatology. 57, 821-836,https://doi.org/10.1175/JAMC-D-17-0157.1 , 2018.

Chen, Q., Yin, Y., Jin, L.-j., Xiao, H., & Zhu, S.: The effect of aerosol layers on convective cloud microphysics and precipitation, Atmos. Res., *101*, 327-340, https://doi.org/10.1016/j.atmosres.2011.03.007, 2011

655 Costantino, L., & Bréon, F.: Analysis of aerosol-cloud interaction from multi-sensor satellite
656 observations, Atmos. Sci., *37*,https://doi.org/10.1029/2009GL041828, 2010
657 Fan, C., Ding, M., Wu, P., & Fan, Y.: The Relationship between Precipitation and Aerosol: Evidence
658 from Satellite Observation, Atmos. Oce. Phy.,https://doi.org/10.48550/arXiv.1812.02036,
659 2018.
660 Feingold, G., Eberhard, W. L., Veron, D. E., & Previdi, M.: First measurements of the Twomey indirect
661 effect using ground-based remote sensors, Geophy. Res. Let., *30*,
662 https://doi.org/10.1029/2002GL016633, 2003.
663 Gryspeerdt, E., Quaas, J., & Bellouin, N.: Constraining the aerosol influence on cloud
664 fraction, *JGR.Atmos*,*121*, 3566-3583,https://doi.org/10.1002/2015JD023744 , 2016.
665 Hassan, M. A., Mehmood, T., Liu, J., Luo, X., Li, X., Tanveer, M., & Abid, M.: A review of particulate
666 pollution over Himalaya region: Characteristics and salient factors contributing ambient PM
667 pollution. Atmos. Envi., 294, 119472, https://doi.org/10.1016/j.atmosenv.2022.119472 , 2002.
668 Hong, Y., Hsu, K. L., Moradkhani, H., & Sorooshian, S.: Uncertainty quantification of satellite
669 precipitation estimation and Monte Carlo assessment of the error propagation into hydrologic
670 response, Wat. Resc. Res., 42, 8, https://doi.org/10.1029/2005WR004398 , 2006.
671 Hossain, F., Anagnostou, E. N., & Bagtzoglou, A.: On Latin Hypercube sampling for efficient
672 uncertainty estimation of satellite rainfall observations in flood prediction, Comp. & geosc., 32,
673 6, 776-792, https://doi.org/10.1016/j.cageo.2005.10.006 , 2006.
674 Jiang, H., Feingold, G., & Cotton, W.: Simulations of aerosol-cloud-dynamical feedbacks resulting from
675 entrainment of aerosol into the marine boundary layer during the Atlantic Stratocumulus
676 Transition Experiment, JGR. Atmos., *107*, AAC 20-1-AAC 20-11,
677 https://doi.org/10.1029/2001JD001502, 2002.
678 Jung, E.: Aerosol-cloud-precipitation interactions in the trade wind boundary layer, Ph.D Thesis,
679 Meteorology and Physical Oceanography, University of Miami, 91-pp., 2012.
680 Kang, N., Kumar, K. R., Yin, Y., Diao, Y., Yu, X.: Correlation analysis between AOD and cloud
681 parameters to study their relationship over China using MODIS data (2003-2013): impact on
682 cloud formation and climate change,AAQR.,*15*, 958-
683 973,https://doi.org/10.4209/aaqr.2014.08.0168 , 2015.
684 Kaskaoutis, D., Kumar Kharol, S., Sinha, P., Singh, R., Kambezidis, H., Rani Sharma, A.: Extremely
685 large anthropogenic-aerosol contribution to total aerosol load over the Bay of Bengal during
686 winter season, Atmos. Chem. Phy., *11*, 7097-7117, https://doi.org/10.5194/acp-11-7097-2011 ,
687 2011.
688 Kedia, S., Ramachandran, S., Holben, B., & Tripathi, S.: Quantification of aerosol type, and sources of
689 aerosols over the Indo-Gangetic Plain,Atmos.Envi.,, *98*, 607-
690 619,https://doi.org/10.1016/j.atmosenv.2014.09.022, 2014.

691 Koike, M., Asano, N., Nakamura, H., Sakai, S., Nagao, T., & Nakajima, T.: Modulations of aerosol
692 impacts on cloud microphysics induced by the warm Kuroshio Current under the East Asian
693 winter monsoon, JGR. Atmos.,*121*,282-297,https://doi.org/10.1002/2016JD025375, 2016.
694 Kubar, T., Hartmann, D., & Wood, R.: Understanding the importance of microphysics and macrophysics
695 for warm rain in marine low clouds. Part I: Satellite observations, Atmos. Sci. 66, 2953-2972,
696 https://doi.org/10.1175/2009jas3071.1, 2009.
697 Kumar, A., & Physics, S.: Variability of aerosol optical depth and cloud parameters over North Eastern
698 regions of India retrieved from MODIS satellite data,Atmos. Sol. Terr. Phy.,*100*, 34-
699 49,https://doi.org/10.1016/j.jastp.2013.03.025, 2013.
700 Kump, L. R., & Pollard, D.: Amplification of Cretaceous Warmth by Biological Cloud Feedbacks, Sci.,
701 *320*, 195-195,https://doi.org/10.1126/science.1153883, 2008.
702 Li, J., Lv, Q., Zhang, M., Wang, T., Kawamoto, K., Chen, S., & Zhang, B.: Effects of atmospheric
703 dynamics and aerosols on the fraction of supercooled water clouds, *Atmos. Chem. Phy.*, *17*,
704 1847-1863,https://doi.org/10.5194/acp-17-1847-2017, 2017.
705 López-Romero, J., Montávez, J., Jerez, S., Lorente-Plazas, R., Palacios-Peña, L., & Jiménez-Guerrero,
706 P.: Precipitation response to aerosol–radiation and aerosol–cloud interactions in regional
707 climate simulations over Europe. *Atmos. Chem. Phys., 21*, 415-430,
708 https://doi.org/10.5194/acp-21-415-2021 , 2021.
709 Masmoudi, M., Chaabane, M., Tanré, D., Gouloup, P., Blarel, L., & Elleuch, F.: Spatial and temporal
710 variability of aerosol: size distribution and optical properties, Atmos. Res., *66*, 1-
711 19,https://doi.org/10.1016/S0169-8095(02)00174-6 , 2003.
712 McCoy, D., Field, P., Schmidt, A., Grosvenor, D., Bender, F., Shipway, B.,& Elsaesser, G.: Aerosol
713 midlatitude cyclone indirect effects in observations and high-resolution simulations, *Atmos.*
714 *Chem. Phy.*, *18*, 5821-5846, https://doi.org/10.5194/acp-18-5821-2018 , 2018.
715 Michibata, T., Kawamoto, K., & Takemura, T.: The effects of aerosols on water cloud microphysics and
716 macrophysics based on satellite observations over East Asia and the North Pacific, Atmos.
717 Chem. Phy., *14*, 10515-10541, https://doi.org/10.5194/acp-14-11935-2014 , 2014.
718 Myhre, G., Stordal, F., Johnsrud, M., Kaufman, Y., Rosenfeld, D., Storelvmo, T.: Aerosol-cloud
719 interaction inferred from MODIS satellite data and global aerosol models, Atmos. Chem. Phy.,
720 *7*, 3081-3101, https://doi.org/10.5194/acp-7-3081-2007, 2007.
721 Nair, V., Giorgi, F., Keshav Hasyagar, U.: Amplification of South Asian haze by water vapour–aerosol
722 interactions, Atmos,Chem.Phy., *20*, 14457-14471, https://doi.org/10.5194/acp-20-14457-2020
723 ,2020.
724 Naud, C., Posselt, D., & van den Heever, S.: Observed covariations of aerosol optical depth and cloud
725 cover in extratropical cyclones, *JGR: Atmos*,*122*,10-
726 338,https://doi.org/10.1002/2017JD027240 , 2017.

727 Rossow, W., & Schiffer, R.: Advances in understanding clouds from ISCCP, Bul. Americ. Meteor. Soci.,
728 *80*, 2261-2288, https://doi.org/10.1175/15200477(1999)080<2261:AIUCFI>2.0.CO;2 ,1999.
729 Sharma, P., Ganguly, D., Sharma, A., Kant, S., Mishra, S.: Assessing the aerosols, clouds and their
730 relationship over the northern Bay of Bengal using a global climate model, Earth. Spac. Sci.,
731 *10*, e2022EA002706, https://doi.org/10.1029/2022EA002706, 2023.
732 Sherwood, S., Roca, R., Weckwerth, T., & Andronova, N.: Tropospheric water vapor, convection, and
733 climate, Rev. of Geophy (AGU), 48, 2,https://doi.org/10.1029/2009RG000301, 2010.
734 Singh, A., Rastogi, N., Sharma, D., Singh, D.: Inter and intra-annual variability in aerosol
735 characteristics over northwestern Indo-Gangetic Plain,AAQR., *15*, 376-
736 386,https://doi.org/10.4209/aaqr.2014.04.0080, 2015.
737 Srivastava, P., Pal, D., Aruche, K., Wani, S., & Sahrawat, K.: Soils of the Indo-Gangetic Plains: a
738 pedogenic response to landscape stability, climatic variability and anthropogenic activity during
739 the Holocene, Earth. Sci. Rew., *140*, 54-71, https://doi.org/10.1016/j.earscirev.2014.10.010,
740 2015.
741 Stevens, B., & Feingold, G.: Untangling aerosol effects on clouds and precipitation in a buffered system,
742 Nature, 461, 607-613,https://doi.org/10.1038/nature08281 , 2009.
743 Sun, J., & Ariya, P.: Atmospheric organic and bio-aerosols as cloud condensation nuclei (CCN): A
744 review, Atmos. Envi., 40, 795-820,https://doi.org/10.1016/j.atmosenv.2005.05.052 , 2006.
745 Tao, W., Chen, J., Li, Z., Wang, C., & Zhang, C.: Impact of aerosols on convective clouds and
746 precipitation, Rev. Geophys., *50*, https://doi.org/10.1029/2011RG000369, 2012.
747 Thomas, A., Kanawade, V., Sarangi, C., & Srivastava, A.: Effect of COVID-19 shutdown on aerosol
748 direct radiative forcing over the Indo-Gangetic Plain outflow region of the Bay of Bengal,Sci.
749 Total Envi., *782*, 146918,https://doi.org/10.1016/j.scitotenv.2021.146918, 2021.
750 Tian, Y., & Peters-Lidard, C.: A global map of uncertainties in satellite-based precipitation
751 measurements, Geohys. Res. Let., 37, 24, https://doi.org/10.1029/2010GL046008 , 2010.
752 Tripathi, S. N., Pattnaik, A., & Dey, S.: Aerosol indirect effect over Indo-Gangetic plain, Atmos.
753 Envi., 41, 33, 7037-7047, https://doi.org/10.1016/j.atmosenv.2007.05.007, 2007.
754 Twomey, S.: The influence of pollution on the shortwave albedo of clouds, Atmos. Sci., *34*, 1149-
755 1152,https://doi.org/10.1175/1520-0469(1977)034<1149:TIOPOT>2.0.CO;2 , 1977.
756 Verma, S., Ramana, M., & Kumar, R.: Atmospheric rivers fueling the intensification of fog and haze
757 over Indo-Gangetic Plains, Sci. Reports., Nature, *12*, 5139, 2022.
758 Wolf, E., & Toon, O.: Controls on the Archean climate system investigated with a global climate model,
759 Astrobiology, *14*, 241-253,https://doi.org/10.1089/ast.2013.1112, 2014.
760 Wood, R.: Relationships between optical depth, liquid water path, droplet concentration, and effective
761 radius in adiabatic layer cloud,University of Washington, *3*, 2006.

762 Wu, P., Dong, X., Xi, B., Liu, Y., Thieman, M., & Minnis, P.: Effects of environment forcing on marine
763 boundary layer cloud-drizzle processes, JGR: Atmos., *122*, 4463-
764 4478,https://doi.org/10.1002/2016JD026326, 2017.
765 Wyant, M., Bretherton, C., Bacmeister, J., Kiehl, J., Held, I., Zhao, M., Soden, B.: A comparison of
766 low-latitude cloud properties and their response to climate change in three AGCMs sorted into
767 regimes using mid-tropospheric vertical velocity, Clim. Dyn., *27*, 261-279,
768 https://doi.org/10.1007/s00382-006-0138-4, 2006.
769 Yuan, T.: Increaseofclouddropletsizewith aerosolopticaldepth: Anobservationandmodelingstudy, JGR:
770 Atmos., *113*, D4, https://doi.org/10.1029/2007JD008632, 2008.
771 *Yang, Y., Liu, X, Qu, Y., An, J., Jiang, R., Zhang, Y., & Ma, Q. : Characteristics and formation*
772 *mechanism of continuous hazes in China: a case study during the autumn of 2014 in the North*
773 *China Plain. ACP., 15, 8165-8178,* https://doi.org/10.5194/acp-15-8165-2015, 2015.
774 Zeb, B., Alam, K., Sorooshian, A., Chishtie, F., Ahmad, I., Bibi, H.: Temporal characteristics of aerosol
775 optical properties over the glacier region of northern Pakistan, Jour. Atmos. Sol-Terr. Phy., *186*,
776 35-46,https://doi.org/10.1016/j.jastp.2019.02.004, 2019.
777 Zhao, C., Tie, X., & Lin, Y.: A possible positive feedback of reduction of precipitation and increase in
778 aerosols over eastern central China, Geo. Res. Let., 33, 11,
779 https://doi.org/10.1029/2006GL025959, 2006.
780 Zhou, S., Yang, J., Wang, W., Zhao, C., Gong, D., Shi, P.: An observational study of the effects of
781 aerosols on diurnal variation of heavy rainfall and associated clouds over Beijing–Tianjin–
782 Hebei, Atmos. Chem. Phy., *20*, 5211-5229,https://doi.org/10.5194/acp-20-5211-2020, 2020.